

1 **A stacked Late Quaternary fluvio-periglacial sequence from the Axe valley,**
2 **Southern England with implications for landscape evolution and Palaeolithic**
3 **archaeology**

4
5 A.G. Brown^{a,*}, L.S. Basell^b, P.S. Toms^c

6
7 ^{a*} Palaeoenvironmental Laboratory University of Southampton (PLUS), School of Geography,
8 University of Southampton, Highfields Campus, Southampton SO17 1BJ, United Kingdom. Tel. 02380
9 595493 Email: Tony.Brown@soton.ac.uk (corresponding author)

10 ^b Geography, Archaeology and Palaeoecology, Queen's University Belfast, Belfast BT71NN, United
11 Kingdom

12 ^c Luminescence dating laboratory, School of Natural and Social Sciences, University of Gloucestershire,
13 Swindon Road, Cheltenham GL50 4AZ, United Kingdom

14
15 **Abstract**

16 The current model of mid-latitude late Quaternary terrace sequences, is that they are uplift-
17 driven but climatically controlled terrace staircases, relating to both regional-scale crustal and
18 tectonic factors, and palaeohydrological variations forced by quasi-cyclic climatic conditions in
19 the 100 K world (post Mid Pleistocene Transition). This model appears to hold for the majority
20 of the river valleys draining into the English Channel which exhibit 8-15 terrace levels over
21 approximately 60-100m of altitudinal elevation. However, one valley, the Axe, has only one
22 major morphological terrace and has long-been regarded as anomalous. This paper uses both
23 conventional and novel stratigraphical methods (digital granulometry and terrestrial laser
24 scanning) to show that this terrace is a stacked sedimentary sequence of 20-30m thickness with
25 a quasi-continuous (i.e. with hiatuses) pulsed, record of fluvial and periglacial sedimentation
26 over at least the last 300-400 K yrs as determined principally by OSL dating of the upper two

27 thirds of the sequence. Since uplift has been regional, there is no evidence of anomalous
28 neotectonics, and climatic history must be comparable to the adjacent catchments (both of
29 which have staircase sequences) a catchment-specific mechanism is required. The Axe is the
30 only valley in North West Europe incised entirely into the near-horizontally bedded chert
31 (crypto-crystalline quartz) and sand-rich Lower Cretaceous rocks creating a buried valley.
32 Mapping of the valley slopes has identified many large landslide scars associated with past and
33 present springs. It is proposed that these are thaw-slump scars and represent large hill-slope
34 failures caused by Vauclausian water pressures and hydraulic fracturing of the chert during
35 rapid permafrost melting. A simple 1D model of this thermokarstic process is used to explore
36 this mechanism, and it is proposed that the resultant anomalously high input of chert and sand
37 into the valley during terminations caused pulsed aggradation until the last termination. It is
38 also proposed that interglacial and interstadial incision may have been prevented by the over-
39 sized and interlocking nature of the sub-angular chert clasts until the Late Glacial when
40 confinement of the river overcame this immobility threshold. One result of this
41 hydrogeologically mediated valley evolution was to provide a sequence of proximal
42 Palaeolithic archaeology over two MIS cycles. This study demonstrates that uplift tectonics and
43 climate alone do not fully determine Quaternary valley evolution and that lithological and
44 hydrogeological conditions are a fundamental cause of variation in terrestrial Quaternary
45 records and landform evolution.

46

47 **Keywords:** periglaciation, incision, chert, thermokarst, Quaternary hydrogeology, hydraulic
48 fracturing, bifaces, Palaeolithic, Acheulian

49

50

51

52 **1. Introduction**

53 The typical configuration of Quaternary fluvial sediment bodies along the NW border of
54 Europe is as river terrace staircases which decrease in age with decreasing altitude (Bridgland
55 and Westaway, 2007) as is seen in the Severn, and Thames (UK: Bridgland et al., 2004), Seine
56 and Somme (France: Antoine et al., 2000) and Middle Rhine (Germany: Westaway, 2002).
57 This scenario would be expected in non-cratonic areas where regional uplift has occurred
58 (Bridgland and Westaway, 2008). For example where, during the Quaternary, river systems are
59 close to glacial margins or within permafrost-affected regions and have been subject to large
60 fluctuations in sediment supply with or without uplift (Hancock and Anderson, 2002). Recent
61 research and sediment dating has shown that this model is frequently complicated by intra-
62 cyclic sediments forming compound terraces of two cold (stadial) phases (although rarely
63 more) separated by channel fills, loess or landsurfaces (e.g. palaeosols) of interstadial or
64 interglacial origin (Lewin and Gibbard, 2010). This staircase configuration is reversed below a
65 hinge-line into subsiding basins, such as the southern North Sea (Rhine) and into lateral
66 diachroneity in tectonically stable areas. Whilst this model was based upon the larger river
67 systems in Europe it also holds for small river systems and for most of the rivers along the
68 coast of England (Brown et al., 2010) and France which drain into the Channel River (English
69 Channel/La Manche; Fig. 1a). The only exception appears to be the River Axe which, as
70 mapped by the British Geological Survey (BGS; Edwards and Gallois, 2004), contains only one
71 terrace at 14-30 m above the Holocene floodplain, small (unmapped) fragments of a lower
72 terrace only 1-2m above the floodplain and spreads of 'head' or solifluction gravels on the
73 upper slopes (Fig. 2). These two gravel bodies make up the Axe Valley Formation (Campbell et
74 al., 1998a) which is known from three quarrying locations Kilmington, Broom and Chard
75 Junction Quarry (henceforth, CJQ). To the west the Otter and Exe valleys (Fig. 1) have
76 altitudinal staircases of 10 and 8 terraces respectively (Edwards and Gallois, 2004; Brown et

77 al., 2009, 2010; Basell et al., 2011) and to the east the Frome/Piddle and Stour systems (Fig. 1)
78 also have altitudinal staircases of 12-15 terraces (BGS 2000) as would be expected in a region
79 that has undergone Quaternary regional-uplift (Westaway, 2010; 2011). The River Axe is also
80 known for a remarkably rich intra-fluvial Lower Palaeolithic site at Broom (Reid Moir, 1936;
81 Hosfield, 2008; Hosfield et al., 2011; Hosfield and Green, 2013) which has produced over 1800
82 bifaces and is only comparable to rivers to the east at Woodgreen on the River Avon, and Red
83 Barns and Hill Head on the Solent River (Wenban-Smith and Hosfield, 2001). This paper
84 presents the results of research at the only working quarry in the Axe valley which had the aim
85 of explaining this anomalous situation (i.e. single compound terrace) and understanding its
86 ramifications for both Quaternary landform evolution and Palaeolithic archaeology.

87

88 **2. Previous Studies**

89 The Axe is one of several catchments which drained into the English Channel and southern
90 North Sea since the breaching of the Weald-Artois anticline; but which lie just to the south of
91 the maximum glacial extent of the British-Irish-Fennoscandian ice sheet (Fig. 1) and
92 experienced periglacial conditions for most of the Late Quaternary (Mol et al., 2000; Renssen
93 and Vandenberghe 2003). The Quaternary evolution of the River Axe has received
94 considerable attention over the last 50 years due to its valley morphology and importance in
95 Palaeolithic archaeology. Its atypical nature (single terrace) was noted by Green (1974; 2013)
96 and Shakesby and Stephens (1984) and one of the aims of these studies was to test the
97 hypothesis first proposed by Mitchell (1960) and later by Stephens (1977) that the anomalously
98 thick gravels resulted from overflow through the Chard Gap (Fig. 3) from a ponded proglacial
99 lake, Lake Maw, in the Somerset Levels (Fig. 1). The gravels at Chard do not support this
100 hypothesis for two reasons. Firstly there are no clasts from the north Somerset area and
101 secondly the gravels continue upstream of the entry point of the Chard gap into the Axe Valley,

102 and into upstream tributaries (Green, 1974; Campbell et al., 1998; Green, 2013). What is
103 certain from these studies is that the Axe Valley and CJQ contains only one major
104 morphological terrace and an anomalously thick sequence of locally derived gravels,
105 principally Upper Greensand chert and flint. OSL dating at Broom also showed that the
106 sequence younged upwards and is therefore a stacked or vertically aggraded gravel body of
107 Late Pleistocene age (Hosfield et al., 2006, 2011). The quarry at Chard Junction which has
108 been operating since the 1950s has produced occasional finds of Palaeolithic artefacts but these
109 were found out of context (not in the gravel faces) such as the twisted ovate found by J. J.
110 Wymer in 1959 and cordiform biface he also found in 1974. Wymer (1999) clearly thought that
111 the site had considerable potential probably due to its proximity to the well-known sites at
112 Broom (Hosfield et al., 2011; Hosfield and Green, 2013). Other than these isolated finds out of
113 sedimentary context there has been no archaeological recording of the sub-surface archaeology
114 of the gravels at Chard Junction (Basell et al., 2007). Palaeolithic artefacts recorded in the
115 county Historic Environment Records (HERs) supplemented by museum records were plotted
116 onto the DEM/geology drape and it can be seen that a cluster of 11 existed in the CJQ area
117 prior to this study (Fig. 2).

118

119 **3. Catchment hydrogeology**

120 The bedrock geology and hydrogeology of the Axe valley are of critical importance to its
121 Quaternary evolution and so will be discussed in some detail. The English Channel cuts
122 discordantly across the Cenozoic basins and axial structures (anticlines) that run from the Seine
123 Basin to the Thames Basin and further west to the Wessex basin and Dorset plateaux (Fig. 1).
124 This provides the well-known laterally time-transgressive Mesozoic section that is known as
125 the Jurassic Coast. This mega-section youngs from the Upper Triassic at the west end
126 (Exmouth Sandstone and Mudstone) to the Upper Cretaceous at the east end (Upper Chalk

127 Group). The Axe catchment is located approximately mid-way along this sequence and is
128 incised into a short outcropping section of mid-Cretaceous Upper Greensand and chalk which
129 form the scarp slopes of the Blackdown Hills (Fig. 1c). The Upper Greensand is a sub-
130 horizontal sequence of clays, weakly- and un-cemented sandstones, and tabular chert overlain
131 by clay-with-flints of Eocene age. Large blocks of siliceous rock known as sarsens, are also
132 found on the Blackdown plateau and it is believed that they are also of Eocene age along with
133 the clay-with-flints formation (Isaac, 1979; Scrivener et al., 2011). The valley has incised
134 through this sequence and is now floored by mudstones of Lower Jurassic age up to just above
135 CJQ at Forde Abbey. This coincides with a nick-point at the upper end of the incised valley
136 (Fig. 3) with the result that the valley-sides below this point are composed of a 120m thick
137 'layer-cake' of clay, sands and chert, sand and a basal mudstone of low permeability. In
138 contrast the catchments to the west are underlain by only sandstones and mudstones (no chert)
139 and to the east by chalk or Palaeogene sediments. A particularly unusual feature is the sand-
140 chert-sand alternation which occurs in the CJQ area at 90 to 160 m OD (metres above ordnance
141 datum sea level) and which produces a lower and upper spring-line at the base of the two
142 sandstone members (Foxmould Member and Bindon Sandstone Member, Fig. 1). These
143 members are separated by mineralised erosion surfaces (hardground) forming hydrogeological
144 discontinuities. Today minor seepage occurs from the upper spring-line but the lower spring-
145 line has historically had enough discharge to power a number of mills and a gravity driven
146 fountain at Forde Abbey. The chert is well exposed 5 km to the east of the Axe valley at
147 Shapwick/Pinhay Quarry where it is a 30m thick bed of cryptocrystalline silicate fractured into
148 tabular bedded blocks along the bedding which varies from 1cm to 40cm in thickness
149 (Eggerton Grit). The quarry also reveals large phreatic tubes towards the base of this member
150 (Brown et al., 2011a).

151

152 **4. Methodology**

153 The research at the recent extraction phases of CJQ (Hodge Ditch Phases I-III) was partly
154 designed to allow the testing of novel techniques with potential for the monitoring of difficult
155 Palaeolithic sites where there is a low density of lithic remains and an unknown potential for
156 environmental information (Brown et al., 2011b). To this end the study involved not only
157 standard lithological recording of gravel faces, but also geomorphological mapping, the
158 analysis of borehole and gamma cps logs, digital granulometry (DG) and terrestrial laser
159 scanning (TLS). Pre-extraction borehole records and gamma cps logs (Slatt et al., 1992) were
160 used to derive a stratigraphic cross-section of the terrace gravels at Hodge Ditch (Fig. 4).
161 Although the lithological descriptions did not reliably distinguish between the sandy gravels
162 and other diamictons it was found that matrix-rich diamicton had a consistently higher relative
163 gamma cps values (50+) allowing its differentiation from chert gravels and sands which both
164 had low gamma cps values (c. 10), due to the inherited mineralogy from the Eocene clays and
165 the mudstones (Brown et al, 2011b). The second novel methodological element of this project
166 was the application of DG. The method is common in the analysis of sediment thin sections and
167 geomorphology (Butler, et al. 2001; Graham et al. 2005a, 2005b; Strom et al. 2010) where it is
168 used for the determination of the grain size distribution of river gravels. The application here
169 uses a commercially available software (Sedimetrics®, Graham et al., 2005b) on vertical faces
170 of gravel to generate grain size distribution curves. A 10 megapixel camera was used (Canon
171 Powershot 10XIS with a 20x optical zoom) give a minimum measurable grain size (MMGS) of
172 approximately 4 mm for a 0.3 m² frame area. Testing has shown that there is a linear
173 relationship between DG results and descriptive results derived from traditional sieving (Brown
174 et al., 2011b; Basell et al. subm.). The TLS system used was a Leica ScanStation HDS3000 at
175 typical ranges of 10-200m. A semi-permanent dGPS grid (using a Leica RX1250Xc GPS &
176 GLONASS SmartRover), was established with a network of 12 temporary benchmark (TBM)

177 targets which allowed any TLS position in the quarry to incorporate at least 3 reference targets.
178 After processing (including cleaning), registration using Leica GeoOffice Combined v7 x,y,z
179 data were exported and input into ArcGIS for solid model rendering used here and
180 experimentally to generate grain size data (Basell et al.subm.).

181
182 All the gravels investigated were fully decalcified due to the acidic nature of the majority of the
183 lithologies making up the catchment and so dating employed OSL initially as part of a wider
184 dating programme of South West British river deposits (Toms et al., 2008, 2013). For the OSL
185 dating, samples were collected in daylight from sections by means of opaque plastic tubing
186 (150 x 45 mm) hammered into each face. In order to attain an intrinsic metric of reliability and
187 where possible, multiple samples were obtained from stratigraphically equivalent units
188 targeting positions likely to be divergent in dosimetry on the basis of textural differences. A
189 measure of γ dose rate was made in situ using an EG&G μ Nomad portable NaI gamma
190 spectrometer. To preclude optical erosion of the datable signal prior to measurement, all
191 samples were prepared under controlled laboratory illumination provided by Encapsulite RB-10
192 (red) filters. Following segregation of material potentially exposed to light during sampling,
193 fine sand sized quartz was isolated by means of acid and alkaline digestion (10% HCl, 15%
194 H₂O₂) to attain removal of carbonate and organic components; a further acid digestion in HF
195 (40%, 60 min) to etch the outer 10–15 nm layer affected by a radiation and degrade each
196 samples' feldspar content; 10% HCl was then added to remove acid soluble fluorides. Each
197 sample was re-sieved and quartz isolated from the remaining heavy mineral fraction using a
198 sodium polytungstate density separation at 2.68 g cm³. Equivalent dose (D_e) values were
199 acquired using a Risø TL-DA-15 irradiation-stimulation-detection system (Markey et al., 1997;
200 Bøtter-Jensen et al., 2003) and single-aliquot regenerative dose protocol (Murray and Wintle,
201 2000; 2003). Optimal thermal treatment was evaluated from measures of D_e and dose recovery

202 preheat dependence. Dose rate (D_r) values were estimated through a combination of *in situ* γ
203 spectrometry (γD_r), Neutron Activation Analysis (βD_r) and geographical position and
204 overburden thickness (Cosmic D_r ; Prescott and Hutton, 1994). Disequilibrium in the U-series
205 was monitored by means of *ex situ* gamma spectrometry using an Ortec GEM-S high purity Ge
206 coaxial detector system.

207

208 **5. Results: Stratigraphy, Sedimentology and Lithology**

209 Borehole logs reveal that the full sequence of deposits on the southern side of Hodge Ditch
210 extends from 79m to 47m OD at the thalweg of the buried valley although only the upper 23m
211 has been exposed by quarrying above the present water table. The general sequence across the
212 entire pit is typically tripartite above the mudstone bedrock head. A pit was dug in the quarry
213 floor to inspect the bedrock-sediment junction at c. 55m OD on the slope of the buried valley,
214 although boreholes indicate that the gravels extend to 47m OD. This pit revealed up to 1m of
215 highly fractured brecciated Charmouth Mudstone (Unit C, Fig. 4g) with a disrupted contact
216 exhibiting festoons and flame structures. Above the junction up to 64.4m OD are horizontally
217 bedded clast-supported medium to well sorted gravels, with occasional shallow cross-bedding
218 which includes trough-bedding varying between a SE to SW flow direction as would be
219 expected in braided river with a N-S orientated valley. Overlying these gravels is a thick but
220 highly variable unit of bedded fine to medium gravels (71-64.5m OD) with the development of
221 large sand-filled channels bisecting the site approximately from east to west. To the north and
222 south the channel is cut into horizontally bedded gravels. The sands display well-developed
223 frost cracks (Fig. 4c), micro-joints and normal faults with minor displacement (Grubbenvorst
224 type *sensu* Mol et al., 1993) and the gravels show features typical of cryoturbation including
225 overturning, *in-situ* shattered clasts and transported angular clasts of silty-sand. These deposits
226 are highly laterally variable as recorded by conventional logging (Fig. 4) and ground laser

227 scanning (Fig. 5). At one location in Hodge Ditch III a thin and reworked slightly organic clay
228 palaeosol was observed (Fig. 4b) smeared-out into a series of pockets and included in
229 cryogenic involutions just below the contact between the sands and the upper diamicton. Above
230 an abrupt but irregular unconformity an upper matrix-rich, massive, poorly sorted, dark-red
231 gravel-rich diamicton formed the sloping superficial unit (unit A in Fig. 4) from 79m to 71m
232 OD at its maximum thickness. This thins from the bedrock valley sides to the NE of the site
233 towards the valley axis. This unit has a high gamma cps values typical of a mixture of the
234 underlying weathered Lower Lias (including Charmouth Mudstones) and chert clasts. TLS of
235 23 faces one of which is shown in Figure 5, were integrated and used to generate a solid model
236 (Fig. 6). Due to the high variability of the gravels both laterally and vertically only the sand
237 channel and the upper diamicton unit are differentiated in this model but it shows a former
238 channel of the Axe buried by renewed gravel deposition prior to the deposition of the palaeosol
239 (Fig. 4) and the diamicton.

240
241 Lithological analysis shows that the clasts throughout are overwhelmingly composed of sub-
242 rounded to angular chert typical of the Whitecliff Chert Member (70-80%) with 30-20% flint
243 although 0-2% of the clasts are quartz, quartzites and metamorphic rocks (Brown et al., 2011b).
244 Some of the chert clasts reach boulder size (>256mm long axis) and are typically sub-angular
245 with one or two faces showing a pre-weathered surface. This 'tabular' chert has probably been
246 derived from fractures and weathered scarp faces on the middle to upper valley-side slopes and
247 has undergone relatively little fluvial transport as the overwhelming majority of clasts were
248 angular to sub-angular (75-80%). The quartzites are all well rounded and originally derived
249 from Palaeozoic sources to the west later incorporated into a conglomerate within the Upper
250 Greensand cherts at Snowdon Quarries, near Chard, or the Trias Pebble Beds (Budleigh
251 Salterton Pebble Beds) which outcrop immediately to the west of the present Axe catchment.

252 Alternatively they could have been derived from an upper plateau gravel. Support for this
253 origin comes from the occurrence of some large pebbles and small boulders with thick grey
254 weathering rinds, solution pits and the occurrence at the site of occasional small ‘sarsens’
255 which are blocks of silicified sandstone (silcretes) found on the Blackdown Plateau (Fig. 4).
256 The grain size envelope reveals the gravels beds to be very poorly sorted medium gravels to
257 cobbles with a secondary mode in the medium-coarse sand sized fraction (-1 phi). The lithic
258 artefacts all fall into the upper part of the range but none lie outside the D₉₅ of the gravel beds.
259 However, the small sarsens lie well outside the gravel range and are therefore very unlikely to
260 have been transported into the reach by fluvial processes. Although the lithic artefacts found
261 prior to and during this research are within the transported size-ranges their condition varied
262 from rolled (highly abraded) to fresh (unabraded with sharp edges).

263

264 **6. Results: archaeology and dating**

265 As part of the ad-hoc monitoring in 2008 two lanceolate bifaces were discovered (2°55'21" W
266 50°50'17" N) in close proximity and from the basal strata of the Hodge Ditch Phase I extraction
267 area (Brown and Basell, 2008). During continued recording of the site a further biface was
268 found during 2008. Further finds included a biface (broken in antiquity), a very small biface
269 (found in 2013), a flake and a core in Hodge Ditch Phase II. Although none of these finds were
270 discovered embedded in a gravel face) they can all be confidently associated with specific areas
271 and stratigraphic units within the pit (Hodge Ditch II) and particular working levels at or below
272 56m OD. They were found in the southern areas of Hodge Ditch I and II and within the lower
273 gravels. These lithics vary from fresh with sharp edges, to moderately rolled and one is
274 unusually large (22 cm length and 1.1 kg in weight) suggesting two-handed use, probably for
275 the butchery of large herbivore carcasses (Schick and Toth, 1993). Given the large quantity of
276 gravels removed from Hodge Ditch I-III (over 1.8 M tons) and frequent monitoring throughout

277 this represents a low ‘background’ density probably related to hominin activity along the
278 floodplain and at the nearby high concentration site at Broom (Hosfield and Green, 2013).

279
280 Thirty three optical age estimates from Hodge Ditch I are outlined in Table 1 and illustrated in
281 Fig. 7. All but four samples (GL08047, GL09117, GL09118, GL10066) have D_e values of less
282 than 600 Gy, the maximum dose so far verified to produce accurate age estimates in the UK
283 (Pawley et al., 2010). Excluding those samples that failed analytical diagnostics (Table 1 and
284 Fig. 7), sedimentation between 55.8m and 66.5m OD appears centred upon a geometric mean
285 age of 259 ± 10 ka (MIS 7). Samples associated with the artefact level (GL08043, GL08044,
286 GL08046 but excluding GL08047) show convergent age estimates from divergent dosimetry
287 (Toms et al., 2005) providing an intrinsic measure of reliability and a weighted mean age of
288 326 ± 22 ka (MIS 9), but this should be considered as a minimum estimate for artefact age.

289
290 Additional dating evidence came from an exposure in Hodge Ditch III in 2011 when quarrying
291 revealed a small lens of dark-grey clay with associated mottling of the underlying sands at 0.8m
292 below the junction with the superficial diamicton. Analysis of the lens revealed it to be a low
293 organic content sandy silty-clay with unidentified small rootlets. Its thinness (1-4 cm) and the
294 minimal soil formation below it (no B horizon), suggest it is a re-worked organic channel fill.
295 Pollen analysis was undertaken on one large sample (100g) and despite the low sample counts
296 (Table 2) it is clear that the assemblage is dominated by tree pollen and particularly *Alnus*. The
297 presence of *Alnus* and other thermophilous trees (*Quercus*, *Fraxinus* and *Corylus*) clearly
298 indicates that this is from an interglacial rather than an interstadial and the presence of
299 *Carpinus* and *Taxus* and the sedimentary context below the upper diamicton unit the most
300 likely ascription is to some time in MIS5 and most likely 5e. The retained fraction from sieving
301 produced very little organic residue and no insect (coleoptera, diptera or chironomid) remains

302 were found. The plant material consisted only of unidentified fine root or stem material
303 probably of monocotyledonous origin, black humic matter and very small lignified fragments
304 of stem. Some small fragments of charcoal were present (under 2mm) and material including a
305 few whole leaves of bryophytes. Comparison with type material and reference to Smith (2004)
306 showed them to be typical of *Sphagnum* sp.. Studies using an environmental scanning electron
307 (ESEM) revealed chains of cubic crystals within carbonised plant tissues within a
308 predominantly quartz matrix. The individual crystals are 0.5-1 micron in size and typical of
309 magnetotactic bacteria that require molecular oxygen to produce magnetic minerals
310 intracellularly in the form of a chain within a magnetosome (Stolz et al., 1990). Microbial
311 activity under conditions of low and alternating redox potential is known to produce both
312 spherules (Ariztegui and Dobson 1996; Brown et al. 2010) and chains (Stolz et al., 1990).
313 Given the lack of soil structure and no B horixon, the carbonised rootlets and the evidence of
314 reducing conditions from the magnetobacteria we conclude that this is the remains of a shallow
315 pool or pond smeared-out probably by the deposition of the overlying sand and gravel and
316 possibly the deposition of the superficial diamicton. It illustrates that there was a hiatus in
317 floodplain aggradation and the floodplain supported at least herbaceous vegetation growing in
318 shallow pools during the last interglacial.

319

320 **7. Discussion: Geomorphological mapping and thermokarst formation**

321 This and other studies in the Axe valley have shown that the vast majority of the compound
322 terrace is locally derived chert from the Whitecliff Member and sand from the Greensand
323 Members (Foxmould and Bindon Sandstone) which outcrop on the valley sides (Fig. 1). Given
324 the thickness of gravels over a reach of approximately 25 km and the stratigraphy of the
325 superficial diamicton geomorphological mapping was undertaken in order to identify proximal
326 chert sources. An area of 6 km² upslope of the diamicton cone and the Hewood Bottom

327 tributary was mapped (Fig. 9). The valley-side slope above the quarry (NW corner of Fig. 9)
 328 which has an average gradient (0.015 m m^{-1}), has a structurally controlled form reflecting the
 329 near horizontal clay-with-flints, sandstone and chert stratigraphy. This produces an upper
 330 plateau, shallow ridges and convex slopes, and lower chert-underlain rectilinear or concave
 331 slopes with alternating spurs and shallow valleys. Descending from the springs along these
 332 valleys are a series of steep sided gullies many of which have pronounced concave headwalls at
 333 or below the springs. These features (Fig. 9 A-E) have arcuate to horseshoe-shaped planforms
 334 and are amphitheatre-like. The most pronounced which is located at the lower spring-line is
 335 187 m across and 5 m deep. They are easily distinguished from quarries by their regular bowl-
 336 shape and locations on spring-lines. These features are remarkably similar to the scars left by
 337 ground-ice slumps or retrogressive thaw-slumps in areas undergoing rapid permafrost melting
 338 (Lewkowicz, 1988; Froese et al., 2008) such as the well-studied examples in the Yukon
 339 (Lantuit et al., 2012) (Fig. 9). Active retrogressive thaw-slumps consist of a steep ($20^\circ - 90^\circ$)
 340 headwall of ice-rich permafrost and a more gentle ($3^\circ - 10^\circ$) foot slope of thawed rock and soil
 341 (Burn and Lewkowicz, 1990) and in planform they can be vary from open-arcuate/D shape to
 342 lemniscate/teardrop shape. These slumps would have fed a slurry of sand and chert directly
 343 onto the floodplain via the tributary.

344 Following from the identification of these features along with many indications of periglacial
 345 conditions affecting the palaeo-floodplain, it was decided to examine the implications of simple
 346 permafrost melt model on these slopes. In order to keep the model requirements as minimal as
 347 possible the model used was the simple surface temperature driven TTOP model (Fig. 10) from
 348 Wright et al. (2003):

349

350
$$TTOP = \frac{K_t K_f (n_t DDT - n_t DDF)}{\dots} \quad \text{Eqn. 1}$$

351
352
353
354
355
356
357
358
359
360
361
362
363
364
365
366
367
368
369
370
371
372
373
374
375

P

Where TTOP is the temperature ($^{\circ}\text{C}$) at the top of the permafrost, K_t is the thermal conductivity of the unfrozen ground, K_f is the thermal conductivity of the frozen ground, DDT is the air thawing index (degree days), DDF is the air freezing index (degree days), n_t is the thawing n-factor (vegetation), n_f is the freezing n-factor (vegetation) and P is the annual period (365 days). From the estimation of TTOP and assuming a linear profile (so assuming a homogenous substrate at that point on the slope) an estimate of permafrost thickness can be calculated by extrapolating along the geothermal gradient to 0°C . The values used were taken from Lebreton et al. (1994) for K_t and K_f but with no correction for soil mineralogy as this has been found to be insignificant in its effect (Riseborough and Smith, 1998). The values used are given in Table 3 and the surface vegetation was assumed to be tundra. TTOP was generated from the estimated mean annual temperature for southern England during the late glacial maximum (Atkinson et al. 1987) and a sinusoidal annual temperature amplitude of 26°C which is slightly higher than a typical value for modern arctic Canada (23° , Wright et al., 2003). When applied using these values the result is a winter permafrost thickness varying from 88m to 122m with lithology (greater on the chert and mudstone and less on the clays and sands) and deep enough to freeze the entire sedimentary sequence outcropping on the slopes (Table 3; Fig. 10). Thawing was rapid and would have been fastest on the sands, and clay with flints. With the deepening of the active layer the sand members would have been saturated but vertical drainage would be prevented by the aquicludes (impermeable rocks) and any remaining permafrost in the chert and mudstones. If thawing of bedrock and soil ice releases water faster than it can drain porewater pressures will rise, effective rock stress fall, and frictional strength is reduced (Morgenstern and Nixon, 1971; Harris et al. 1995). The result would high pore-water pressures within the sand units and the chert, and very high seepage pressures at both the upper and lower

376 spring-line. Given the impermeable nature of the chert this may have caused hydraulic
377 fracturing of the chert, reduced frictional strength and induced slope failure. In other words,
378 ideal conditions for thaw-slump generation at these points on the slopes, with the resultant mass
379 failure of sand and chert in the form of debris-flows and slumps with shear planes in the lower
380 saturated Foxmould sand over the Gault and Eype Clay. Under this scenario the chert would be
381 transported as coarse clasts within a saturated sand matrix in non-Newtonian flows even on low
382 slopes, here typically 1-2°. These debris flow injections onto the floodplain (similar to the
383 upper diamicton) were reworked and sorted by the river until MIS 4-2 when the river was
384 confined by the debris-cone on the north side of the floodplain and incised through the gravel
385 stack. Reworking of the debris flows must have taken place when the surface was unfrozen
386 including under interstadial and interglacial periods. This is a process-based version of the
387 ‘fluvioperiglacial’ models of both Castleden (1980), Bryant (1983) and Shakesby and Stephens
388 (1984) and explains the anomalous accumulation of gravels from the Upper Greensand slopes
389 down to the buried valley at the present river mouth (Fig. 3). A possible alternative model
390 could be active layer saturation causing the retrogressive thaw slumps during full periglacial
391 conditions, however, these would not be located at the bedrock junctions/springs, and the well-
392 developed melt features (including the smeared-out palaeosol) below the upper diamicton
393 support our view that the driver is melting of the permafrost at terminations (*sensu* Broecker
394 and van Donk, 1970; Denton et al. 2010).

395

396 **8. Discussion: Terrace formation**

397 Combining the stratigraphy and the OSL dating we suggest that the uppermost unit at Chard
398 Junction Quarry is solifluction and thaw-slump derived debris-flow deposits which
399 accumulated during the Devensian post MIS 5a. The uppermost OSL dates on the underlying
400 bedded sand and gravel suggest accumulation during the early Devensian MIS 5a-d and an

401 MI5e date for the organic deposits is consistent with the palynology. The middle bedded units
402 of bed D appear to have accumulated in cold stages MIS 6 and this is in agreement with the
403 sedimentological evidence of freezing of the floodplain surface. These sediments closely
404 resemble the periglacial alluviation model of Bryant (1983) with an abundant supply of sand
405 and chert gravel deposited as medial and lateral bars in a braided channel-system. The lowest
406 accessible beds (i.e. those above the present water table) may pre-date MIS 7 but confirmation
407 of this is underway using post-IR IRSL dating (Thomsen et al., 2008). The gravel-bedrock
408 contact shows strong development of brecciation which is interpreted here and elsewhere in
409 southern England as being due to permafrost ice-segregation and which made bedrock
410 vulnerable to thermal erosion (Murton and Lautridou, 2003; Murton and Belshaw, 2011). It
411 follows that the incision of the buried valley within which this sediment stack has accumulated
412 was pre MIS 9-10. It is most likely that this deep, buried valley from CJQ to the coast
413 represents incision to the low Mid-Pleistocene sea level during MIS 12 (Fig. 2). This
414 accommodates additional incision of the English Channel River due to breaching (Gupta et al.,
415 2007). This does not conform to the standard model (Bridgland and Westaway, 2007;
416 Bridgland, 2000) and we suggest this is because the Upper Greensand being highly erodible
417 was deeply incised in the early Pleistocene and incision, although slowed once the mudstones
418 were encountered, was after MIS 12, prevented by sediment oversupply and the nature of the
419 chert as bed material. It is also possible that a threshold for incision reached after MIS 12 was
420 not reached again until the termination of the last glacial cycle.

421
422 This study has confirmed that the lithic artefacts discovered at Chard come from the basal 10m
423 of the sequence and that the site has a low or background-level density, but that the lithics have
424 probably not travelled far from their point of discard. At Broom, and particularly the Ballast or
425 Railway Pit the stratigraphy and the archaeology differs significantly from that at Chard. In

426 particular at Broom there is the development of a laterally extensive pollen-bearing clays and
427 silts or a subaerial loam that was deposited in a temperate stage possibly during an interstadial
428 within MIS 8, or in MIS 9 (Hosfield et al., 2011; Hosfield and Green, 2013) and this is not the
429 case at CJQ which is a more active reach. The archaeology, which was an initial justification
430 for the study, is also different because the total number of finds from Chard is c. 23 (including
431 local surface finds), while Broom produced over 1800 stone tools. The concentration at Broom
432 probably represents nearby chert knapping activity and artefact use very close to the final
433 depositional context. This can be contrasted with the low density lithics at CJQ, which probably
434 represent discard or loss following transport to, or use at, locations not far from the shores of a
435 palaeo-river Axe. This study shows that the massive difference in artefact numbers is due to the
436 hominin behavioural patterns rather than the geomorphological contexts of the sites. The
437 majority of the bifaces at Broom are ovates and cordates, although pointed forms are known,
438 the biface finds reported here are similar being lanceolate (corresponding to Hosfield and
439 Chamber's "pointed" categorization) and cordate in form. Our research suggests that the
440 artefact-bearing gravels at CJQ are broadly contemporaneous with the assemblage at Broom
441 although at neither site has it been possible to directly date a bed containing an *in-situ* artefact
442 assemblage. This confirms that Broom is a 'super-site' probably due to the reworking into the
443 channel of a proximal archaeological context, possibly even a biface pavement (Brown et al.,
444 2013).

445
446 Taken together the sites at CJQ, Broom and Kilmington reveal episodic cold-stage
447 fluvioperiglacial aggradation during the Middle-Late Pleistocene. In being a stacked sequence
448 the Axe Valley is exceptional in southern England and this requires explanation. The typical
449 geophysical context for terrace staircases is relative uplift with repeated down-cutting to low
450 base levels as provided by cold-period sea levels whereas stacked sequences are typical of

451 subsiding basins such as the lower Rhine sequence under the Netherlands (Peeters et al., 2014).
452 Although the area is affected by faults which may have been active into the Quaternary
453 (Gallois, 2006) there is no evidence that the Axe valley was part of a subsiding block relative to
454 the catchments each side of it. Indeed the whole Blackdown block, SW peninsula and South
455 Coast has undergone variable uplift during the Quaternary (Westaway, 2010; 2011). It is also
456 self-evident that the climate of this catchment must have been similar to its surrounding areas
457 throughout the Quaternary. An alternative explanation is that the catchment has, at some stage
458 in the later Quaternary, been reduced in size by river capture, thus reducing its discharge but
459 not reducing the sediment input from main valley slopes. Such a possibility has been postulated
460 by Gallois (2006) with capture of part of the adjacent proto-Otter by the Exe/Culm system but
461 this did not affect the Axe catchment. Shakesby and Stephens (1984) suggested that high rates
462 of sediment availability and periglacial transport produced the thickened Axe Valley Formation
463 and Hosfield and Green et al (2013) stress the erodible nature of the Upper Greensand
464 lithologies. Whilst this is undoubtedly correct we argue this is not enough, as similar conditions
465 pertained in the adjacent Otter Valley and the rivers draining the north and eastern edges of the
466 Blackdown Plateau, all of which exhibit terrace staircases. The mapping of the slopes above
467 Chard Junction suggest that the entire catchment was highly susceptible to thermokarstic melt-
468 out processes at terminations due fundamentally to its layered stratigraphy of highly
469 permafrost-sensitive rocks i.e. sand with fractured chert over a basal aquiclude. The
470 pronounced spring-lines of the hills is seen largely as a relic of the operation of a pressurised
471 groundwater system during periglacial melting and associated retrogressive thaw-slumping.
472 Modelling has suggested that the occurrence of pressurised groundwater systems was common
473 in northwest Europe in areas of discontinuous permafrost including river valleys and would
474 have had its maximum effect in lithologies with high effective porosities and permeabilities
475 (van Weert et al., 1997).

476

477 The pre-fractured nature of the chert and the bimodal grain size of sediment (cobbles vs fine-
478 medium sand) may also be important for the lack of incision between stadials until the later
479 Devensian. The pre-fractured chert forms sub-angular blocks of cubic to tetrahedron shape
480 which after winnowing of the sand matrix have a tendency to lock together forming a
481 pavement, especially as upstream bedload input reduces (Dietrich et al., 1989). A simple
482 calculation using the grain size distribution envelope (Fig. 8) of the Shields stress required to
483 move the D_{50} of the gravels and the D_{95} suggests a 44% higher critical shear stress would be
484 required to disrupt an armoured bed and this takes no account of any imbrication and
485 interlocking which would increase this value further. Armouring and the thick gravel body
486 would have increased hyporheic flow during temperate conditions and reduced the likelihood
487 of bed incision. This mechanism is supported by the high lateral variability of the gravels
488 formed as a result of laterally shifting channels and bars and the common occurrence of small
489 lenses of framework gravels. The Devensian incision took place prior to the deposition of the
490 lower inset terrace. Although not dated in this study it is comparable in height and extent with
491 the lowest terrace in the Exe system which has been dated to the Late Glacial stadial (Younger
492 Dryas; Bennett et al., 2011). The sloping surface of the terrace throughout the valley suggests
493 the possibility that the solifluction/debris flow unit was so extensive that it confined the channel
494 to a small part of the floodplain. This would have promoted incision when vegetation had
495 stabilised valley slopes although this process may have started as hyporheic flow, in a
496 depressed thaw zone under the floodplain under warming climate conditions (Zarnetske, et al.,
497 2008; Murton and Belshaw, 2011). This mechanism may also provide an explanation for the
498 prior incision of the valley floor which initiated the stacked sequence post MIS 12 as suggested
499 by the bedrock brecciation. It must also have been important in increasing the erodibility of

500 bedrock at floodplain edges thus facilitating lateral expansion of the braidplain and what has
501 been termed in the past fluvio-periglacial pedimentation *sensu* Castleden (1980).

502

503 **10. Conclusions**

504 1. The chronostratigraphic data presented in this paper reveals that the Axe, a tributary valley
505 of the Channel River in southern England, has undergone quasi-continuous fluvial aggradation
506 - with hiatuses and lateral reworking - from MIS 10 and possibly MIS 12 until MIS 2 when it
507 underwent an incision and then a minor aggradational phase. The sediment-stack up to 32m in
508 total thickness is preserved in one major compound terrace with a sloping surface formed by
509 debris-flow deposits which is particularly well-developed at tributary junctions.

510 2. This morphology and developmental history is in stark contrast to all the other fluvial
511 systems draining into the English Channel/La Manche system in southern England and northern
512 France which are all terrace staircase systems regarded as typical of non-cratonic areas close to
513 Quaternary glacial margins. Such an anomaly requires an explanation within or outside the
514 current conceptual model of terrace formation. However, the Axe is also unusual in being
515 entirely incised into a near-horizontally bedded alternating sequence of weakly cemented sands
516 and cherts over mudstones of Mesozoic age. Geomorphological mapping of the valley slopes
517 has revealed features along prominent spring-lines which on morphological grounds are very
518 similar to modern retrogressive thaw slumps found in areas of melting permafrost.

519 3. A simple 1D model (TTOP) is used to test this hypothesis and it suggests that that permafrost
520 differentially melted in non-cemented sands both below and above the chert beds producing a
521 pressurised groundwater system which instigated hydraulic fracturing of the chert and
522 retrogressive thaw slumping. This liberated the pre-fractured chert in debris-flows providing a
523 high input of both sub-angular chert within fluidized sand onto the floodplain. This input was
524 locally reworked by fluvial activity but not incised into until the Late Glacial. The reasons for

525 this change in fluvial behaviour are not known but may be due to a combination of the
526 confinement of the river by debris flow deposits and thermokarst induced down-cutting after
527 reduced sediment supply.

528 4. One result of this hydrogeologically mediated valley evolution was the preservation of a
529 record of both proximal (near-site) and background Lower Palaeolithic hominin activity in the
530 form of lithic artefacts. The similarity between the artefact typologies at CJQ and nearby
531 Broom and the OSL dating at both sites suggests a common age of either MIS 9 or 7, and the
532 low-density of artefacts at CJQ confirms the importance of Broom as a ‘super-site’ (*sensu*
533 Ashton and Hosfield 2010 and Brown et al. 2013) and its likely proximity to an *in-situ*
534 assemblage reworked into an adjacent channel.

535 5. Most importantly this study demonstrates that uplift tectonics and climate alone do not fully
536 determine Quaternary valley evolution and that lithological and hydrogeological conditions are
537 a fundamental cause of variation in terrestrial Quaternary records.

538

539 **Acknowledgements**

540 The authors must thank all employees of Bardon Aggregates (Aggregate Industries Ltd.) who
541 have assisted this work in every possible way and in particular Tony Pearson, the site manager.
542 We must also thank Buzz Busby, Vanessa Straker and Jonathan Last of English Heritage for
543 their help and encouragement. The research was funded by English Heritage under grant Nos.
544 PNUM 3847 and 5695. This work has benefited from both unpublished data and discussions
545 with Rob Hosfield, Chris Green, Rick Shakesby, Hugh Prudden and many members of the
546 British Quaternary Research Association who visited the site in 2011. Finally, thanks to the two
547 anonymous reviewers for their thought provoking comments.

548

549

550 **References**

551 Antoine, P., Lautridou, J. P. and Laurent, M. 2000. Long-term archives in NW Europe:
552 response of the Seine and Somme rivers to tectonic movements, climatic variations and sea-
553 level changes. *Geomorphology* 33, 183-207.

554

555 Ariztegui, D., & Dobson, J., 1996. Magnetic investigations of framboidal greigite formation; a
556 record of anthropogenic environmental changes in eutrophic Lake St Moritz, Switzerland. *The*
557 *Holocene* 6, 235–241.

558

559 Ashton, N. M. and Hosfield, R. T. 2010. Mapping the human record in the British early
560 Palaeolithic: Evidence from the Solent river system. *Journal of Quaternary Science* 25, 737-
561 753.

562

563 Atkinson, T.C., Briffa, K. R. and Cooper, G. R. 1987 Seasonal temperatures in Britain during
564 the past 22,000 years reconstructed using beetle evidence. *Nature* 325, 587-592.

565

566 Basell, L. S., Brown, A. G. and Hosfield, R. T. 2007. *The Palaeolithic Rivers of South-West*
567 *Britain (PNUM 3847). Fieldwork Report (Phase II)*. English Heritage, London/ADS York,
568 <http://www.personal.rdg.ac.uk/~sgs04rh/SWRivers/Fieldwork%20Report.pdf>

569

570 Basell, L.S., Brown, A. G. and Neild, J. (Subm.) The use of terrestrial laser scanning for the
571 monitoring and sedimentological investigations of an artefact-bearing fluvial sequence in
572 Southern England. *Journal of Archaeological Science*

573

574 Basell, L. S., Brown, A. G., Toms, P. S. and Gallois, R. 2011. The Otter valley gravels and
575 Budleigh Salterton. In L. S. Basell, A. G. Brown and P. S. Toms (Eds.) *The Quaternary of the*
576 *Exe Valley and Adjoining Area. Field Guide*. Quaternary Research Association, London, 139-
577 147.

578

579 Bennett, J. A., Brown, A. G. and Basell, L. S. 2011. Late Pleistocene and Holocene deposits in
580 the Netherex area. In L. S. Basell, A. G. Brown and P. S. Toms (Eds.) *The Quaternary of the*
581 *Exe Valley and Adjoining Area. Field Guide*. Quaternary Research Association, London, 67-76.

582

583 Bøtter-Jensen, L., McKeever, S.W.S. and Wintle, A.G. 2003. *Optically Stimulated*
584 *Luminescence Dosimetry*. Elsevier, Amsterdam.

585

586 Broecker, W. S. and Van Donk, J. 1970 *Reviews of Geophysics and Space Physics* 8, 169–197.

587

588 Bridgland, D.R., 2000. River terrace systems in North West Europe: an archive of
589 environmental change, uplift and early human occupation. *Quaternary Science Reviews* 19,
590 1293–1303.

591

592 Bridgland, D. R. and Westaway, R. 2007. Climatically controlled river terrace staircases: a
593 worldwide Quaternary phenomenon. *Geomorphology* 98, 285-315.

594

595 Bridgland, D. R. and Westaway, R. 2008. Climatically controlled river terrace staircases: a
596 worldwide Quaternary phenomena. *Geomorphology* 98, 285-315.

597

598 Bridgland, D.R., Schreve, D.C., Keen, D.H., Meyrick, R., and Westaway, R., 2004.

599 Biostratigraphical correlation between the late Quaternary sequence of the Thames and key
600 fluvial localities in Central Germany. *Proceedings of the Geologists Association* 115, 125–140.
601
602 British Geological Survey. 2000. *Dorchester, England and wales Sheet 328. Solid and Drift,*
603 *1:50,000.* British Geological Survey, Keyworth, Nottingham.
604
605 Brown, A. G. and Basell, L. S. 2008. New Lower Palaeolithic finds from the Axe Valley,
606 Dorset. *PAST* 60, 1-4.
607
608 Brown, A. G., Ellis, C. and R. Roseff, R. 2010. Holocene sulphur-Rich palaeochannel
609 sediments: Diagenetic conditions, magnetic properties and archaeological implications. *J. of*
610 *Archaeological Science* 37, 21-29.
611
612 Brown, A. G., Basell, L. S., Toms, P. S. and Scrivener, R. C. 2009. Towards a budget approach
613 to Pleistocene terraces: preliminary studies using the River Exe in South West England.
614 *Proceedings of the Geologists' Association.* 120, 275-281.
615
616 Brown, A. G., Basell, L.S, Toms, P.S., Bennett, J., Hosfield, R.T. and Scrivener, R.C. 2010.
617 Late Pleistocene Evolution of the Exe Valley. A Chronostratigraphic Model of Terrace
618 Formation and its Implications for Palaeolithic Archaeology. *Quaternary Science Reviews* 29,
619 897-912.
620
621 Brown, A. G., Powell, M., and Basell, L. S. 2011a. Recent work at Shapwick Grange Quarry
622 and the Blackdown Hills Plateau. In L. S. Basell, A. G. Brown and P. S. Toms (Eds.) *The*
623 *Quaternary of the Exe Valley and Adjoining Area. Field Guide.* Quaternary Research
624 Association, London, 128-132.

624 Brown, A. G., Toms, P. S. and Basell, L. S. 2011b. Monitoring and modelling of the
625 Palaeolithic archaeological resource at Chard Junction Quarry, Hodge Ditch Phases II & III.
626 PNUM 5695. English Heritage Report, ADS York.

627

628 Brown, A. G., Basell, L. S., Robinson, S. and Burdge, G. C. 2013. Site Distribution at the Edge
629 of the Palaeolithic World: A Nutritional Niche Approach. *PLoS ONE* 8(12), e81476, 1-14.

630

631 Bryant, I. D. 1983. Facies sequences associated with some braided river deposits of late
632 Pleistocene age from Southern Britain. In *Modern and ancient fluvial systems*. J. D. Collinson
633 and J. Lewin. Oxford, Blackwell Scientific Publications, 267-275.

634

635 Burn, C.R., and Lewkowicz, A.G. 1990. Retrogressive thaw slumps. *The Canadian*
636 *Geographer* 34, 273–276.

637

638 Butler, J. B., S. N. Lane, and J. H. Chandler. 2001. Automated extraction of grain-size data
639 from gravel surfaces using digital image processing. *Journal of Hydraulic Research* 39, 519-
640 529.

641

642 Campbell, S, Scourse, J.D., Hunt, C.O., Keen, D.H. and Stephens, N. 1998a. *Quaternary of*
643 *South-west England*. Geological Conservation Review Volume, Chapman and Hall, London.

644

645 Campbell, S., Stephens, N., Green, C.P. and Shakesby, R. A. 1998b. Broom gravel pits. In
646 *Quaternary of South-West England*, Campbell, S., Hunt, C.O., Scourse, J.D., Keen, D.H. and
647 Stephens, N. (eds). Geological Conservation Review series, Vol. 14 Chapman & Hall: London;
648 307–318.

649

650 Castleden, R., 1980. Fluvioglacial pedimentation: a general theory of fluvial valley
651 development in cool temperate lands, illustrated from western and central Europe. *Catena* 7,
652 135–152.

653

654 Denton, G. H., Anderson, R. F., Toggweiler, J. R., Edwards, R. L., Schaefer, J. M., Putnam, A.
655 E. 2010. The Last Glacial Termination. *Science*, 1652-1656.

656

657 Dietrich, W. E., Kirchner, J. W., Ikeda, H. and Isega, H. 1989. Sediment supply and the
658 development of coarse surface layers in gravel-bedded rivers. *Nature* 340, 215-217.

659

660 Edwards, R.A. and Gallois, R. W. 2004. *A brief description of the geology of the Sidmouth*
661 *district. British Geological Survey Sheet Explanation. Sheets 326/340 (England and Wales)*

662

663 Froese, D. G., Estgate, J. A., Reyes, A., Enkin, R. J. and Preece, S. J. 2008. Ancient permafrost
664 and future, warmer Arctic. *Science* 321, 1648.

665

666 Gallois, R.W. 2006. The evolution of the rivers of east Devon and south Somerset, UK.
667 *Geoscience in south-west England* 11, 205-213.

668

669 Gardiner V. and Dackombe, R. 1983. *Geomorphological field manual*. George Allen & Unwin,
670 London.

671

672 Graham, D. J., Reid, I. and Rice, S. P. 2005a. Automated sizing of coarse-grained sediments:
673 image-processing procedures. *Mathematical Geology*, 37, 1-28.

674

675 Graham, D. J., Rice, S. P. and Reid, I. 2005b A transferable method for the automated grain
676 sizing of river gravels. *Water Resources Research* 41, 1-12.

677

678 Green, C. P. 1974. Pleistocene gravels of the River Axe in south-western England, and their
679 bearing on the southern limit of glaciation in Britain. *Geological Magazine* 111, 213-220.

680

681 Green, C.P. 2013. Broom and the Axe Valley in the Middle Pleistocene. In Hosfield, R. and
682 Green, C. P. (Eds.) *Quaternary History of Palaeolithic Archaeology in the Axe valley at*
683 *Broom, South West England*. Oxbow, Oxford, 165-169.

684

685 Gupta, S., Collier, J. S., Palmer-Felgate, A. and Potter, G. 2007. Catastrophic flooding origin
686 of shelf-valley systems in the English Channel. *Nature* 448, 342-345.

687

688 Hancock, G.S., Anderson, R.S., 2002. Numerical modelling of fluvial strath-terrace formation
689 in response to oscillating climate. *Geological Society of America Bulletin*, 114, 1131–1142.

690

691 Harris, C., Davies, M. C. R. and Coutard, J-P. 1995. Laboratory simulation of periglacial
692 solifluction: significance of porewater pressures, moisture contents and undrained shear
693 strengths during soil thawing. *Permafrost and Periglacial Processes* 6, 293-311.

694

695 Hosfield, R.T. 2008. Stability or flexibility? Handaxes and hominins in the Lower Palaeolithic.
696 In: Papagianni, D., Maschner, H. and Layton, R. (eds.) *Time and Change: Archaeological and*
697 *Anthropological Perspectives on the Long Term*. Oxbow Books, Oxford, 15-36.

698

699 Hosfield, R. and Green, C. P. (Eds.) 2013. *Quaternary History of Palaeolithic Archaeology in*
700 *the Axe valley at Broom, South West England*. Oxbow, Oxford.

701

702 Hosfield, R. T., Brown, A. G., Basell, L., Hounsell, S. and Young, R. 2006. *The Palaeolithic*
703 *Rivers of South-West Britain. Final Report Phases I & II*. English Heritage, London.

704 Hosfield, R. T., Green, C., Toms, P., Scourse, J. Scaife, R. and Chambers, J. 2011. The Middle
705 Pleistocene deposits and archaeology at Broom. In L. S. Basell, A. G. Brown and P. S. Toms
706 (Eds.) *The Quaternary of the Exe and Adjoining Areas. Field Guide*. Quaternary Research
707 Association, London, 103-127.

708

709 Isaac, K. P. 1979. Tertiary silcretes of the Sidmouth area, east Devon. *Proceedings of the*
710 *Ussher Society* 4, 341-354.

711

712 Lantuit, H., Pollard, W. H., Couture, N., Fritz, M., Meyer, H. and Hubberten, H-W. 2012.
713 Modern and late Holocene retrogressive thaw slump activity on the Yukon coastal plain and
714 Herschel Island, Yukon Territory, Canada. *Permafrost and Periglacial Processes* 23, 39-51.

715

716 Lebret, P., Dupas, A., Clet, M., Coutard, J-P., Lautridou, J-P., Courbouleix, S., Garcin, M. and
717 Levy, M. 1994. Modelling of permafrost thickness during the late glacial stage in France:
718 preliminary results. *Canadian Journal of earth Sciences* 31, 959-968.

719

720 Lewkowicz, A. G. 1988. Slope processes. In M. J. Clark (Ed.) *Advances in Periglacial*
721 *Geomorphology*, Wiley, Chichester 325-368.

722

723 Lewin, J. and Gibbard, P. 2010. Quaternary river terraces in England: Forms, sediments and
724 processes. *Geomorphology* 120, 293-311.

725 Markey, B.G., Bøtter-Jensen, L., and Duller, G.A.T. 1997. A new flexible system for
726 measuring thermally and optically stimulated luminescence. *Radiation Measurements*, 27, 83-
727 89.

728

729 Mitchell, C. F. 1960. The Pleistocene history of the Irish Sea. *Advancement of Science*, 17, 313-
730 25.

731

732 Mol, J., Vandenberghe, J., Kasse, K. and Stel, H. 1993. Periglacial microjointing and faulting
733 in Weichselian fluvio-aeolian deposits. *Journal of Quaternary Science* 8, 15-30.

734

735 Mol, J., Vandenberghe, J., and Kasse, C. 2000. River response to variations of periglacial
736 climate in mid-latitude Europe. *Geomorphology* 33, 131-148.

737

738 Morgenstern, N. R. and Nixon, J. F. 1971. One dimensional consolidation of thawing soils.
739 *Canadian Geotechnical Journal* 11, 447-469.

740

741 Murray, A.S. and Wintle, A.G. 2000. Luminescence dating of quartz using an improved single-
742 aliquot regenerative-dose protocol. *Radiation Measurements*, 32, 57-73.

743

744 Murray, A.S. and Wintle, A.G. 2003. The single aliquot regenerative dose protocol: potential
745 for improvements in reliability. *Radiation Measurements*, 37, 377-381.

746

747 Murton, J. B. and Belshaw, R. K. 2011. A conceptual model of valley incision, planation and
748 terrace formation during cold and arid permafrost conditions of Pleistocene southern England.
749 *Quaternary Research* 75, 385-394.
750

751 Murton, J. B. and Lautridou, J-P., 2003. Recent advances in the understanding of Quaternary
752 periglacial features of the English Chanel coastlands. *Journal of Quaternary Science* 18, 301-
753 307.
754

755 Pawley, S.M., Toms, P.S., Armitage, S.J., Rose, J. (2010) Quartz luminescence dating of
756 Anglian Stage fluvial sediments: Comparison of SAR age estimates to the terrace chronology
757 of the Middle Thames valley, UK. *Quaternary Geochronology* 5, 569-582.
758

759 Peeters, J., Busschers, F.S. and Stouthamer, E. 2014. Fluvial evolution of the Rhine during the
760 last interglacial-glacial cycle in the southern North Sea basin: A review and look forward.
761 *Quaternary International*
762

763 Prescott, J.R. and Hutton, J.T. (1994) Cosmic ray contributions to dose rates for luminescence
764 and ESR dating: large depths and long-term time variations. *Radiation Measurements*, 23, 497-
765 500.
766

767 Reid Moir, J. 1936. Ancient Man in Devon. *Proceedings of the Devon Archaeological*
768 *Exploration Society* 2, 264-275.
769

770 Renssen, H. and Vandenberghe, J. 2003. Investigation of the relationship between permafrost
771 distribution in NW Europe and extensive winter-sea ice cover in the North Atlantic Ocean
772 during the cold phases of the last Glaciation. *Quaternary Science Reviews* 22, 209-223.
773

774 Riseborough, D. W. and Smith, M. W. 1998. Exploring the limits of permafrost. In A. G.
775 Lewkowicz and M. Allard (Eds.), *Permafrost: Seventh International Conference, Yellowknife,*
776 *Canada*, 935-942.
777

778 Scrivener, R. C., Basell, L. S. and Brown, A. G. 2011. Sarsens associated with river terrace
779 gravels in the Creedy valley, Devon. In L. S. Basell, A. G. Brown and P. S. Toms (Eds.) *The*
780 *Quaternary of the Exe Valley and Adjoining Area. Field Guide.* Quaternary Research
781 Association, London, 128-132.
782

783 Schick, K. and Toth, N. 1993. *Making Silent Stones Speak: Human Evolution and the Dawn of*
784 *Technology.* Simon & Schuster, New York.
785

786 Shakesby, R. A. and Stephens, N. 1984. The Pleistocene gravels of the Axe Valley, Devon.
787 *Report of the Transactions of the Devon Association for the Advancement for Science* 116, 77-
788 88.
789

790 Slatt, R. M., Jordan, D. W., D'Agostino, A. E. & Gillespie, R. H. 1992 Outcrop gamma-ray
791 logging to improve understanding of subsurface well log correlations. *Geological Society,*
792 *London, Special Publications* 65, 3-19.
793

794 Smith, A. J. E. 2004. *The Moss Flora of Britain and Ireland. Second Edition.* Cambridge
795 University Press, Cambridge.
796

797 Stephens, N. 1977. The Axe Valley. In D. N. Mottishead (Ed.) *INQUA Congress Guidebook*
798 *for Excursions A6 and C6. South-west England.* Geo Abstracts, Norwich, 24-29.
799

800 Stolz, J.F., Lovley, D.N., Haggerty, S.E., 1990. Biogenic magnetite and the magnetisation of
801 sediments. *Journal of Geophysical Research* 95, 4355–4361.
802

803 Strom, K. B., Kuhns, R. D. & Lucas, H. J. 2010. Comparison of automated image-based grain
804 sizing to standard pebble-counting. *Journal of Hydraulic Engineering* 136, 461-474.
805

806 Thomsen, K.J., Murray, A.S., Jain, M. and Bøtter-Jensen, L. 2008. Laboratory fading rates of
807 various luminescence signals from feldspar-rich sediment extracts. *Radiation Measurements*,
808 43, 1474–1486
809

810 Toms, P.S., Brown, A.G., Basell, L.S. and Hosfield, R.T. (2008) *Palaeolithic Rivers of south-*
811 *west Britain: Optically Stimulated Luminescence dating of residual deposits of the proto-Axe,*
812 *Exe, Otter and Doniford.* English Heritage Research Department Report Series, 2-2008.
813

814 Toms, P.S., Brown, A.G., Basell, L.S., Duller, G. and Schwenninger, J-L. (2013) *Chard*
815 *Junction Quarry, Somerset. Optical Stimulation Luminescence Dating of the Proto-Axe.*
816 *Scientific Dating Report.* English Heritage Research Department Report Series, no. 7-2013.
817

818 Wymer, J. J. 1999. The Lower Palaeolithic Occupation of Britain. Wessex Archaeology and
819 English Heritage, London.

820

821 Van Weert, F. H. A., van Gijssel, K., Leijnse, A., and Boulton, G. S. 1997. The effects of
822 Pleistocene glaciations on the geohydrological system of Northwest Europe. *Journal of*
823 *Hydrology* 195, 137-159.

824 Wenban-Smith, F. F. and Hosfield, R. T. (Eds.) 2001. *Palaeolithic Archaeology of the Solent*
825 *River*, Lithic Studies Occasional paper No. 7, London.

826 Westaway, R. 2002. Geomorphological consequences of weak lower continental crust, and its
827 significance for studies of uplift, landscape evolution, and the interpretation of river terrace
828 sequences. Netherlands. *Journal of Geosciences* 81, 283–304.

829 Westaway, R. 2010. Cenozoic uplift of southwest England. *Journal of Quaternary Science* 25,
830 419–432.

831

832 Westaway, R. 2011. Quaternary fluvial sequences and landscape evolution in Devon and
833 Somerset. In L. S. Basell, A. G. Brown and P. S. Toms (Eds.) *The Quaternary of the Exe*
834 *Valley and Adjoining Area. Field Guide. Quaternary Research Association, London, 27-46.*

835

836 Wright, J. F., Duchesne and Côté, M. M. 2003. Regional-scale permafrost mapping using the
837 TTOP ground temperature model. In Phillips, M. Springman, S.M. and Arenson, L.U. (Eds.)
838 *Permafrost*. Swets and Zeitinger, Lisse. 1241-1246.

839

840 Zaenetske, J. P., Gooseff, M. N., Bowden, W. B., Greenwald, M. J. and Brosten, T. R. 2008.
841 Influence of morphology and permafrost dynamics on hyporheic exchange in Arctic headwater
842 streams under warming climate conditions. *Geophysical Research Letters* 35, L02501.
843
844

845 **Tables**

846

847 Table 1. Dose Rate (D_r), Equivalent Dose (D_e) and Age data of samples from Hodge Ditch I-III
848 (51°N , 3°W , 75 m O.D.). Uncertainties in age are quoted at 1σ confidence, are based on
849 analytical errors and reflect combined systematic and experimental variability and (in
850 parenthesis) experimental variability alone. All ages are expressed in thousands of years before
851 2010.

852

853 Table 2. Pollen count data from large sub-sample from the Hodge Ditch III organic silty clay.

854

855 Table 3. Parameters used in TTOP modelling of permafrost freezing.

856

857

858 **Figure captions**

859

860 Fig. 1. (a) Location of the Axe valley catchment in southern England with catchments coded by
861 the number of BGS terraces recognised (after Brown et al., 2009) and ice limits, (b) generalised
862 geological section of the Jurassic Coast, (b) a simplified geological cross-section along the
863 Jurassic Coast with the Axe valley shown, and (c) a GIS derived drape of the superficial
864 geology of the Axe catchment. Data derived from BGS mapping.

865

866 Fig. 2. Drape of Quaternary deposits, archaeological (Palaeolithic) finds and sites mentioned in
867 the text over a DEM derived from IFSAR data.

868

869 Fig. 3. The long profile is re-drawn using some data from Campbell et al. (1998b), Basell et al.,
870 (2007), Brown et al. (2010) and this paper. Only the OSL dates with no analytical caveats are
871 plotted for CJQ. Upper stippling is Upper Greensand lithologies and below Triassic Mudstones
872 with the junction generalised from BGS mapping.

873

874 Fig.4. Generalised stratigraphic section from CJQ Hodge Ditch Phases 1-3 with insets of
875 sedimentological features (a) upper diamicton unit, (b) organic-rich clay in upper part of Unit
876 B, (c) channel sands with frost cracks between unit B and C, (d) sand lenses within Unit C, (e)
877 clast-supported horizontally bedded gravels in Unit C, (f) a sarsen from Unit B showing surface
878 weathering pits, (g) the brecciated and disrupted bedrock-gravels interface in Hodge Ditch II.

879

880 Fig. 5. Scanned face of a section in with Scan data draped Hodge Ditch 3 with photos taken
881 using the ScanStation and then processed using different image texture settings (upper gamma
882 2 and lower using a colour classification of the intensity of return).

883

884 Fig. 6. (A) HD I, II and III point data interpolated in ArcMap 10 using inverse distance eighting
885 and displayed using height colour values. Displayed in ArcMap (2D) using a pseudo-3D image.
886 Red high, blue low. Red points show distribution of OSL locations labelled according to GL-
887 number. (B) Model with OSL sample locations (black), bedrock from bore hole data, location
888 of one of the scanned faces (pale mauve) inserted from scanned grid co-ordinates as an
889 example, palaeosol (bright pink line in HD3) and location of major sand units derived from
890 scan data and photographs. Artefact locations are shown in bright pink. The apparent position
891 of some of the OSL sample locations within mounds of gravel is because following standard
892 gravel extraction during which samples were taken and sections recorded, the area was

893 subsequently used to dump spoil mounds which were captured by a later scan. 5 x vertical
894 exaggeration.

895

896 Fig. 7. Age depth model derived from OSL and bio-correlation dates. Solid red line signifies the depth
897 of the thin palaeosol. Dashed grey line indicates the level at which artefacts were found. Diamonds
898 represent OSL age estimates, with red fill used to highlight those with analytical caveats. The blue line
899 shows the oxygen isotope curve from ODP 677 along with temperate (red numbered) and cool (blue
900 numbered) MIS.

901

902 Fig. 8. Grains size envelope for CJQ fluvial gravels from Hodge Ditch I-III with moment
903 statistics and size range of the bifaces found during this research.

904

905 Fig.9. GIS DEM of the mapped area around the CJQ showing spring-related thaw-slump
906 landforms (marked by break of slopes as mapped and by symbols A-E). The map uses standard
907 geomorphological symbols as recommended by the Geological Society Engineering Working
908 Party (1972) and reproduced in Gardiner and Dackombe (1983).

909

910 Fig. 10. Simplified model of para-fluvioperiglacial sediment input forced by permafrost
911 melting of the Upper Cretaceous (Greensand) lithological sequence, (a) model representation,
912 (b) the valley-side cross-sectional geology used in the model with present water table and (c)
913 the model with frozen layer and flowlines after sequential melting.

914

Table 1

Lab Code	Overburden (m)	Grain size (μm)	Moisture content (%)	α D _r (Gy.ka ⁻¹)	β D _r (Gy.ka ⁻¹)	γ D _r (Gy.ka ⁻¹)	Cosmic D _r (Gy.ka ⁻¹)	²²⁶ Ra/ ²³⁸ U	Total D _r (Gy.ka ⁻¹)	Preheat (°C for 10s)	D ₀ (Gy)	Age (ka)
GL06010	4.3	125-180	16 ± 4	-	1.09 ± 0.10	0.34 ± 0.02	0.11 ± 0.01	1.25 ± 0.27	1.54 ± 0.10	240	268.5 ± 22.0	174 ± 18 (16)
GL06011	2.5	125-180	13 ± 3	-	0.53 ± 0.04	0.29 ± 0.01	0.14 ± 0.01	0.76 ± 0.12	0.96 ± 0.05	260	90.2 ± 6.8	94 ± 9 (7)
GL06012	1.7	125-180	14 ± 3	-	1.28 ± 0.11	0.53 ± 0.02	0.16 ± 0.02	1.07 ± 0.22	1.97 ± 0.11	260	193.7 ± 11.0	98 ± 9 (6) ^{a,b}
GL06013	4.5	125-180	15 ± 4	-	0.72 ± 0.07	0.26 ± 0.01	0.10 ± 0.01	0.96 ± 0.25	1.09 ± 0.07	240	298.6 ± 19.2	274 ± 25 (20)
GL06057	6.7	125-180	16 ± 4	-	0.75 ± 0.07	0.20 ± 0.01	0.08 ± 0.01	1.04 ± 0.17	1.02 ± 0.07	240	375.3 ± 24.6	367 ± 35 (29)
GL06058	7.0	125-180	15 ± 4	-	0.84 ± 0.08	0.21 ± 0.01	0.07 ± 0.01	0.78 ± 0.12	1.12 ± 0.08	280	318.3 ± 33.3	284 ± 36 (32)
GL08043	15.3	125-180	17 ± 4	-	0.54 ± 0.05	0.22 ± 0.01	0.03 ± 0.00	0.88 ± 0.16	0.80 ± 0.6	280	284.9 ± 31.9	355 ± 47 (43) ^c
GL08044	15.2	125-180	21 ± 5	-	1.22 ± 0.13	0.38 ± 0.02	0.03 ± 0.00	1.03 ± 0.14	1.63 ± 0.14	280	477.2 ± 45.1	292 ± 37 (33)
GL08045	12.9	125-180	17 ± 4	-	0.97 ± 0.09	0.26 ± 0.01	0.03 ± 0.00	0.99 ± 0.16	1.26 ± 0.10	280	332.7 ± 23.8	264 ± 28 (23) ^c
GL08046	15.0	125-180	20 ± 5	-	1.04 ± 0.11	0.48 ± 0.02	0.03 ± 0.00	1.00 ± 0.12	1.56 ± 0.11	260	521.4 ± 41.5	334 ± 36 (31)
GL08047	15.5	125-180	20 ± 5	-	1.03 ± 0.11	0.42 ± 0.02	0.03 ± 0.00	0.79 ± 0.09	1.49 ± 0.11	280	736.8 ± 51.7	494 ± 50 (43) ^{c,d}
GL09029	3.3	125-180	13 ± 3	-	0.54 ± 0.05	0.41 ± 0.02	0.12 ± 0.01	0.87 ± 0.16	1.07 ± 0.05	260	132.1 ± 7.0	124 ± 9 (7) ^e
GL09030	8.1	125-180	13 ± 3	-	0.53 ± 0.05	0.22 ± 0.01	0.06 ± 0.01	0.87 ± 0.22	0.82 ± 1.43	250	247.4 ± 18.9	302 ± 29 (25) ^c
GL09031	9.6	125-180	15 ± 4	-	1.09 ± 0.10	0.28 ± 0.01	0.05 ± 0.01	0.91 ± 0.12	1.43 ± 0.10	230	419.8 ± 31.7	294 ± 30 (26) ^c
GL09117	11.8	5-15	21 ± 5	0.38 ± 0.04	1.44 ± 0.14	0.81 ± 0.03	0.04 ± 0.00	1.21 ± 0.14	2.67 ± 0.15	210	928.1 ± 64.8	347 ± 31 (28) ^d
GL09118	11.7	5-15	19 ± 5	0.35 ± 0.04	1.48 ± 0.14	0.79 ± 0.03	0.04 ± 0.00	0.83 ± 0.10	2.67 ± 0.15	250	614.0 ± 30.6	230 ± 17 (14) ^d
GL09119	8.8	5-15	19 ± 5	0.35 ± 0.04	1.23 ± 0.12	0.61 ± 0.02	0.06 ± 0.01	1.07 ± 0.14	2.26 ± 0.12	260	529.9 ± 24.5	235 ± 17 (14)
GL09120	10.7	125-180	8 ± 2	-	0.59 ± 0.04	0.24 ± 0.01	0.05 ± 0.00	0.90 ± 0.16	0.88 ± 0.05	240	419.1 ± 41.5	475 ± 53 (48) ^e
GL10001	2.6	180-250	9 ± 2	-	0.57 ± 0.04	0.46 ± 0.02	0.14 ± 0.01	0.88 ± 0.14	1.17 ± 0.05	280	164.9 ± 15.6	141 ± 14 (14) ^b
GL10002	13.1	180-250	13 ± 3	-	0.51 ± 0.05	0.31 ± 0.02	0.04 ± 0.00	1.05 ± 0.24	0.86 ± 0.05	240	229.4 ± 16.2	268 ± 25 (21)
GL10013	13.1	125-180	21 ± 5	-	0.50 ± 0.05	0.27 ± 0.01	0.04 ± 0.00	0.96 ± 0.30	0.80 ± 0.06	240	279.4 ± 18.0	348 ± 34 (14) ^c
GL10014	12.9	125-180	12 ± 3	-	0.56 ± 0.05	0.31 ± 0.02	0.04 ± 0.00	0.97 ± 0.25	0.91 ± 0.05	260	284.4 ± 34.1	313 ± 42 (21) ^b
GL10015	14.7	125-180	16 ± 4	-	1.02 ± 0.10	0.50 ± 0.02	0.03 ± 0.00	1.13 ± 0.16	1.55 ± 0.10	260	298.3 ± 30.2	192 ± 23 (40) ^b
GL10016	14.8	125-180	18 ± 4	-	0.84 ± 0.08	0.37 ± 0.02	0.03 ± 0.00	0.98 ± 0.13	1.24 ± 0.09	260	257.7 ± 19.0	208 ± 21 (44)
GL10019	13.0	125-180	15 ± 4	-	0.82 ± 0.08	0.20 ± 0.01	0.04 ± 0.00	0.99 ± 0.17	1.06 ± 0.08	240	262.5 ± 37.9	249 ± 40 (38) ^c
GL10020	14.1	125-180	15 ± 4	-	0.92 ± 0.08	0.35 ± 0.02	0.03 ± 0.00	0.93 ± 0.12	1.30 ± 0.09	240	366.8 ± 37.2	281 ± 34 (31) ^{b,c}
GL10055	13.2	125-180	6 ± 2	-	0.52 ± 0.04	0.28 ± 0.01	0.04 ± 0.00	-	0.84 ± 0.04	260	281.7 ± 21.2	335 ± 31 (26) ^b
GL10063	12.6	125-180	19 ± 5	0.32 ± 0.04	1.33 ± 0.13	0.17 ± 0.01	0.04 ± 0.00	0.98 ± 0.12	1.85 ± 0.13	240	592.7 ± 38.5	320 ± 31 (27)
GL10064	14.8	125-180	11 ± 3	-	0.56 ± 0.05	0.26 ± 0.01	0.03 ± 0.00	0.95 ± 0.24	0.85 ± 0.05	240	180.4 ± 9.5	212 ± 17 (13) ^c
GL10065	12.6	125-180	17 ± 4	-	0.78 ± 0.08	0.41 ± 0.02	0.04 ± 0.00	0.98 ± 0.19	1.24 ± 0.08	240	280.0 ± 17.5	226 ± 20 (17) ^c
GL10066	13.2	125-180	17 ± 4	-	1.11 ± 0.12	0.72 ± 0.08	0.04 ± 0.00	1.17 ± 0.16	1.87 ± 0.15	240	627.2 ± 58.1	336 ± 42 (38) ^{a,d}
GL10067	9.3	125-180	17 ± 4	-	0.98 ± 0.09	0.27 ± 0.01	0.06 ± 0.01	1.01 ± 0.16	1.31 ± 0.10	240	384.8 ± 50.1	293 ± 44 (41) ^c
GL10084	4.4	125-180	19 ± 5	-	0.62 ± 0.05	0.49 ± 0.02	0.10 ± 0.01	1.01 ± 0.16	1.21 ± 0.06	240	152.1 ± 10.4	126 ± 11 (9) ^a

Analytical Caveats: ^aSignificant feldspar contamination, ^bFailed dose recovery test, ^cFailed repeat dose ratio test, ^dD₀ exceeds 600 Gy, ^ePotential partial bleaching, ^fLimited sample mass

Type	CHD3A	%TLP	Gr ml ⁻¹	Comments (provenience)
Trees				
<i>Betula</i>	16	6.3	120	Pioneer gap & floodplain tree (DI)
<i>Pinus</i>	13	5.1	97	Some in the greater region, perhaps in hill tops
<i>Picea</i>	3	1.2	22	Long-distance transport?
<i>Corylus</i>	18	7.1	135	Local understorey & gap tree
<i>Quercus</i>	6	2.4	144	Slope woodland
<i>Alnus</i>	62	24.6	465	Riparian corridor, local to site
<i>Fraxinus</i>	28	11.1	210	Slope woodland
<i>Taxus</i>	1	+	7	Slope of floodplain isolated trees
<i>Carpinus</i>	5	1.9	37	Slope woodland
Total Trees	134	53.1	1005	Floodplain surrounded by woodland
Shrubs				
<i>Salix</i>	6	2.4	45	Floodplain
<i>Hedera</i>	7	2.7	52	On floodplain & slope trees
Total shrubs	13	5.1	97	(note <i>Corylus</i> incl. in tree group)
Herbs				
Poaceae	48	19.0	360	Open parts of the floodplain
Cyperaceae	20	7.9	150	Floodplain & riparian zone
<i>Cannabis</i> t.	1	+	7	On floodplain, open areas (DI)
<i>Centaurea cyanus</i>	2	+	14	On floodplain, open areas
Chenopodiaceae	4	1.5	30	On floodplain or slopes, open areas (DI)
<i>Filipendula</i>	1	+	7	On floodplain, open areas
Lactuceae	1	+	7	On floodplain, open areas (DI)
<i>Plantago lanc.</i>	5	1.9	37	On floodplain or slopes, open areas (DI)
Rubiaceae	2	+	14	On floodplain or slopes, open areas (DI)
<i>Rumex acetosa</i>	2	+	14	On floodplain or slopes, open areas (DI)
<i>Sanguisorba</i>	1	+	7	On floodplain or slopes, open areas (DI)
<i>Thalictrum</i>	1	+	7	On floodplain or slopes, open areas
Total herbs	87	34.1	652	High enough to indicate definite open areas (around site)
Spores				
<i>Polypodium</i>	3	1	7	Slope woodland
Unid.	8	3.1	60	Moderately high – mostly oxidation damage
Charcoal >50µ	21	-	157	Typical distribution for background (natural) fires
Charcoal >25-50µ	84	-	630	
Charcoal <25µ	73	-	547	
Exotics	3333	-	-	-
Total land pollen	252	100	1890	Low concentration due to oxidation/reduction
Total pollen + spores	255	101	1891	

Table 2 Pollen count data from large sub-sample from the Hodge Ditch III organic silty clay.

Climatic parameter	LGM c. 20-16 Ka BP	Rock type	K_t (W m °C)	K_f (W m °C)	Est. thickness of permafrost (m)
Mean annual Temp (°C)	-10	Clay with flints	1.7	2.5	88
Summer max. (°C)	+10	Sand	0.8	0.9	115
Winter min. (°C)	-16	Chert	3.4	3.6	122
Annual amplitude (°C)	26°	Mudstone	1.2	1.3	119
n_t (tundra)	0.67	Mean	-	-	111
n_f (tundra)	0.83				

Table 3. Input and estimated parameters for Chard valley TTOP-based permafrost thickness estimation. Climatic data for LGM takes from Atkinson et al. (1987) with geotechnical estimates from Lebret et al. (1994).

Figure 1

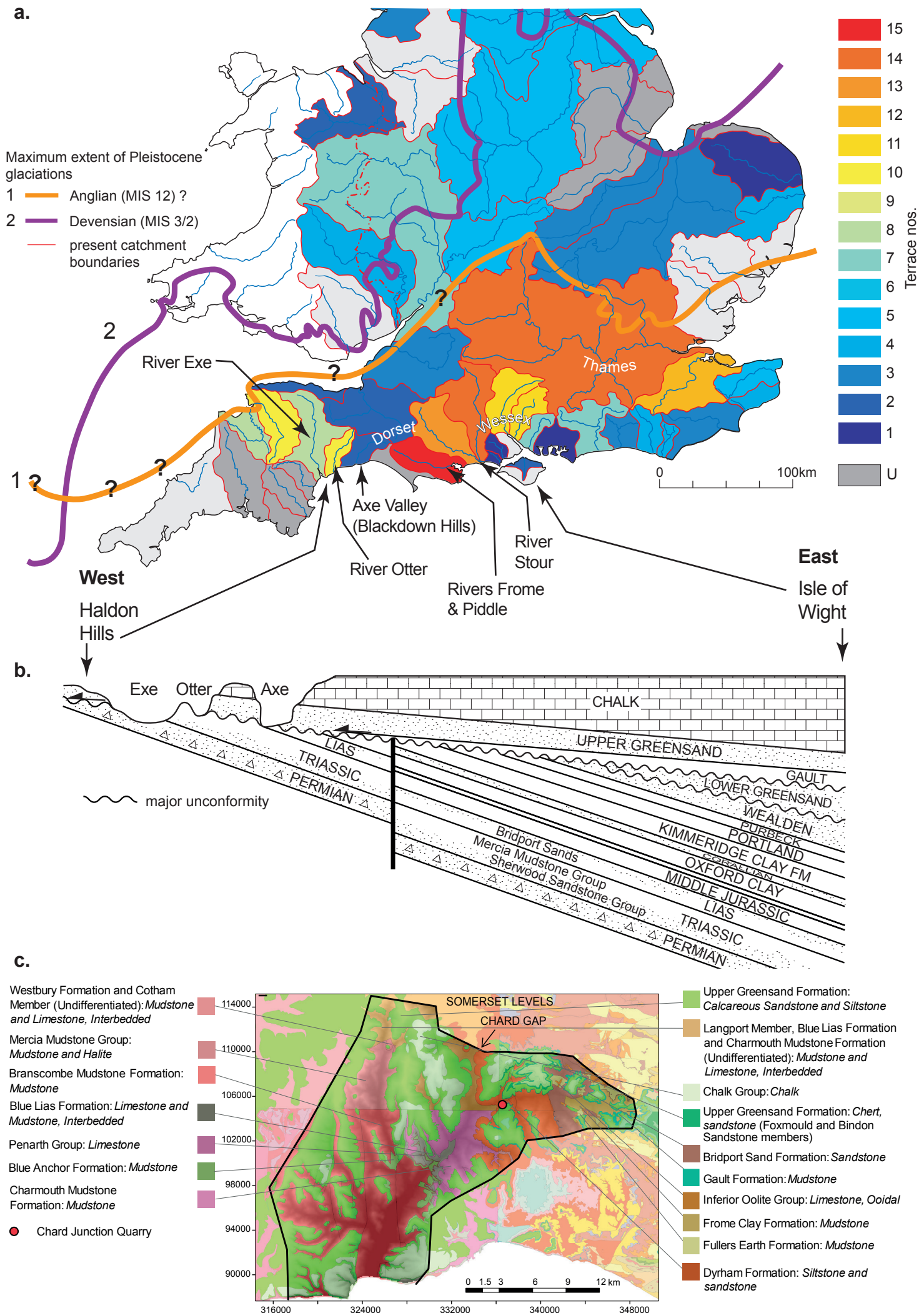


Figure 2

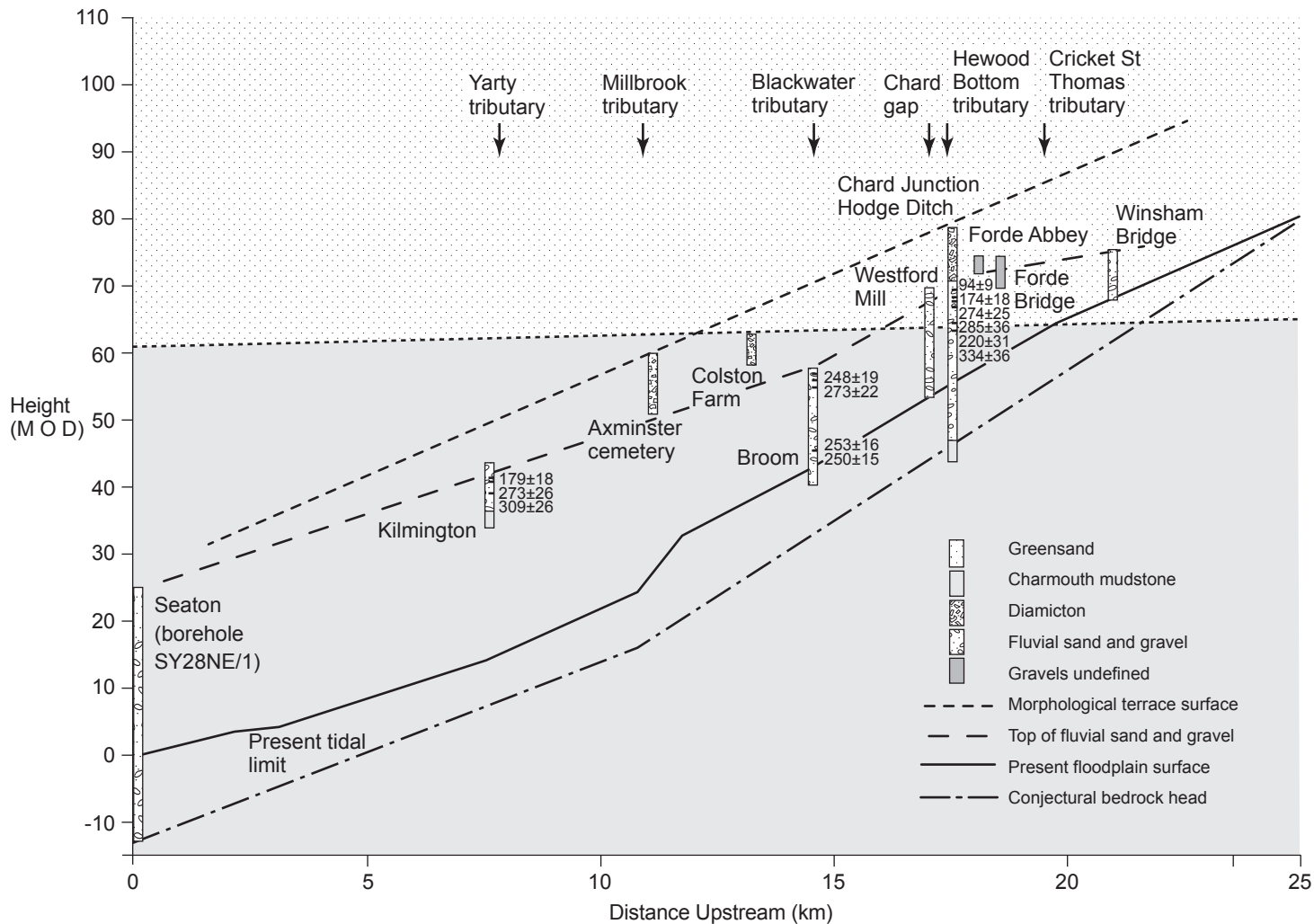


Figure 3

MIDDLE AXE VALLEY DIGITAL ELEVATION MODEL
DRAPED WITH SUPERFICIAL DEPOSITS, PALAEOLITHIC
ARCHAEOLOGICAL FINDSPOTS AND PROSWEB
FIELDWORK LOCATIONS

Topography at x 2 vertical exaggeration

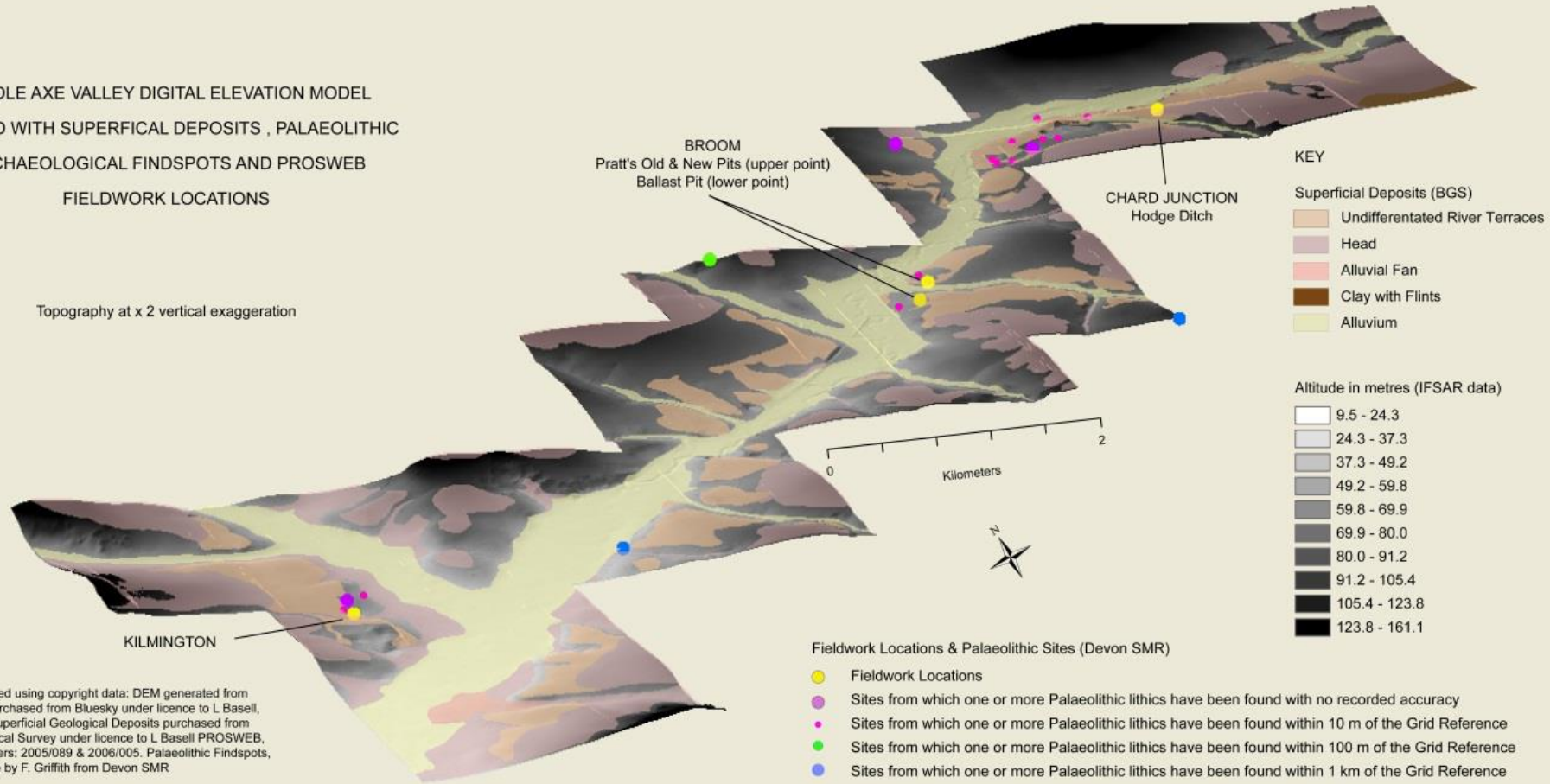
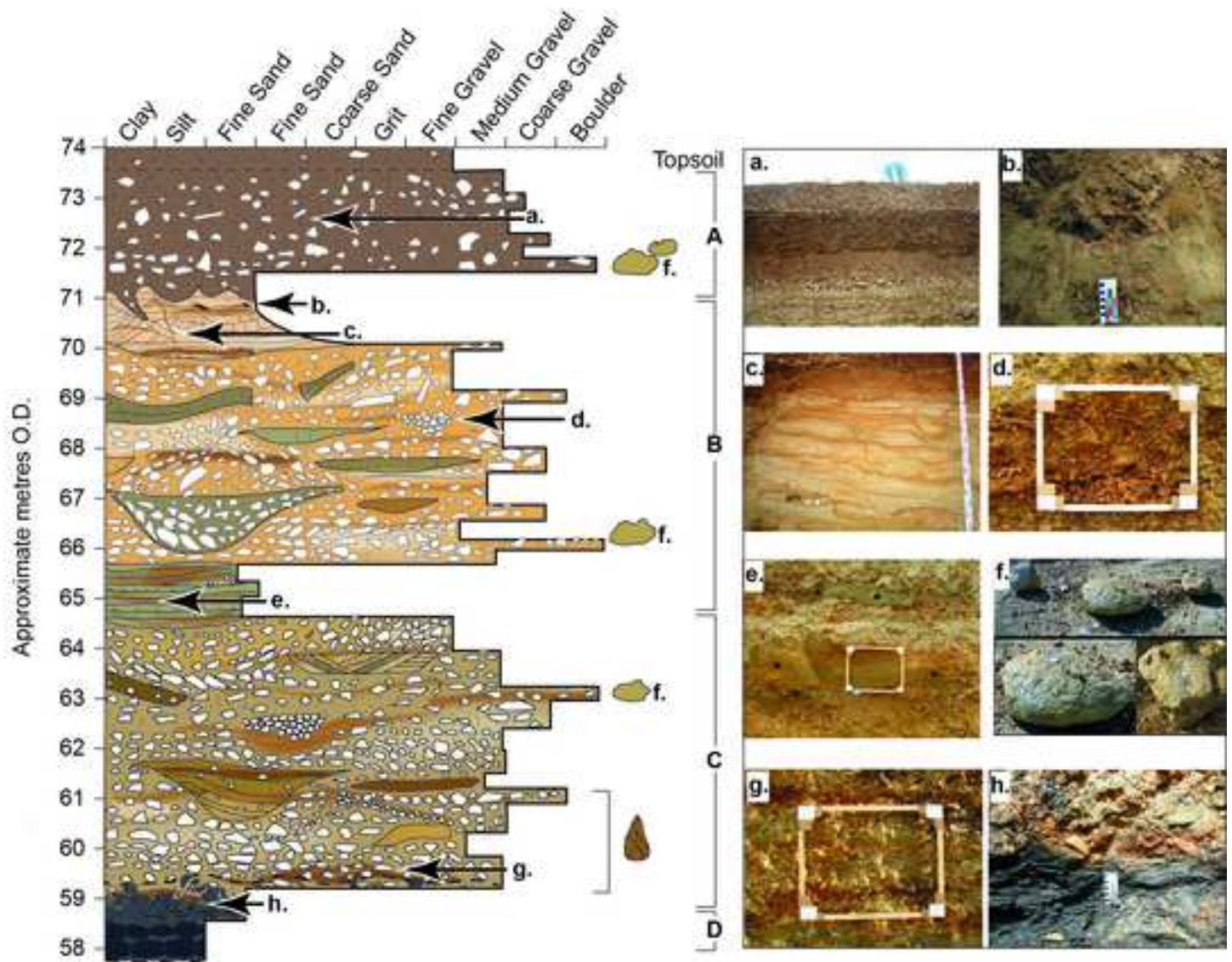


Image generated using copyright data: DEM generated from IFSAR data purchased from Bluesky under licence to L Basell, PROSWEB. Superficial Geological Deposits purchased from British Geological Survey under licence to L Basell PROSWEB, Licence Numbers: 2005/089 & 2006/005. Palaeolithic Findspots, made available by F. Griffith from Devon SMR

Figure 4

[Click here to download high resolution image](#)



Clay	Framework Gravel	Clay Drape	Bifaces	Photographs Small coloured scale = 10cm Frame (internal corners of white squares) = 65cm x 50cm a = ~9-10m (section length) c = ~1m 80cm (height)
Silt	Weathered Charmouth Mudstone, Gravel, Sand, Silt and Clay	Frost Crack	Sarsens	
Sand	Charmouth Mudstone	Diffuse Boundary		
Clasts		Palaeosol		
		Limit of Excavation		

Figure 5

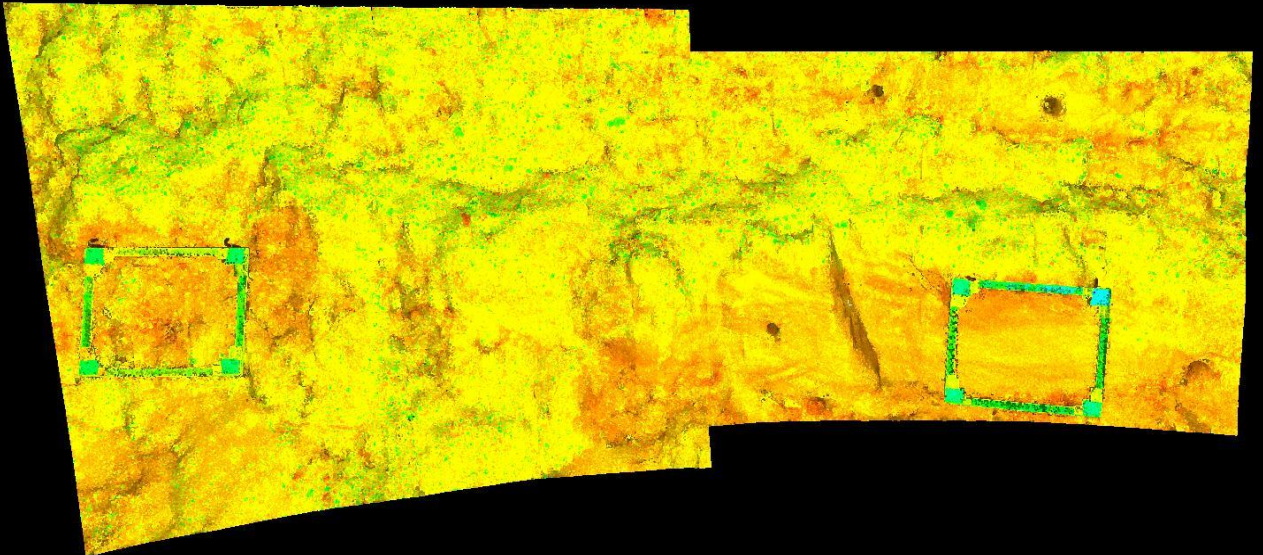
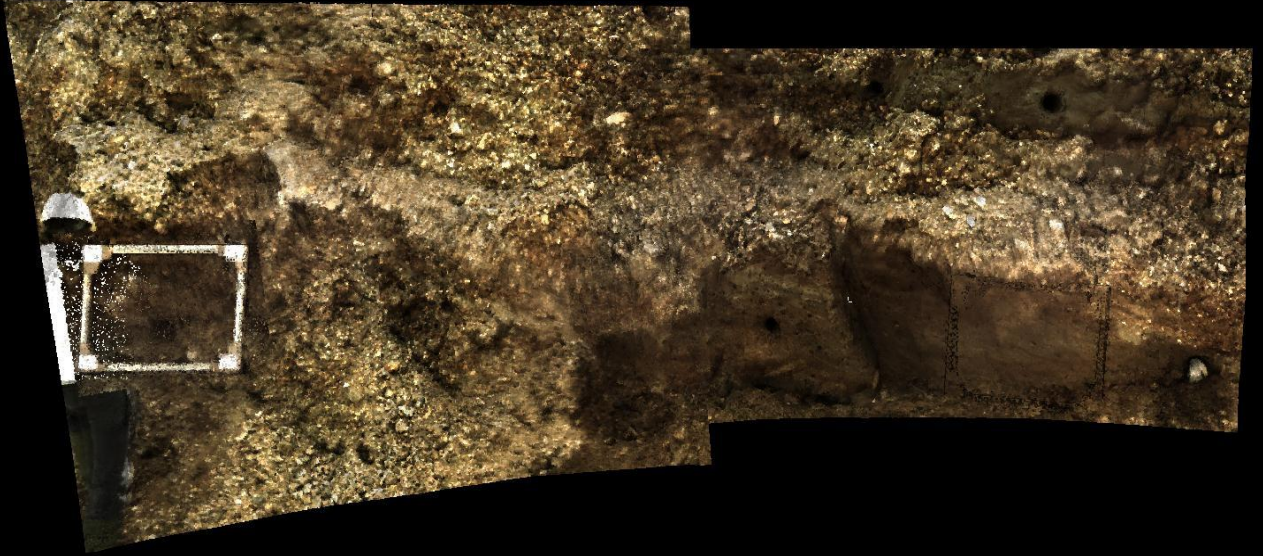


Figure 7

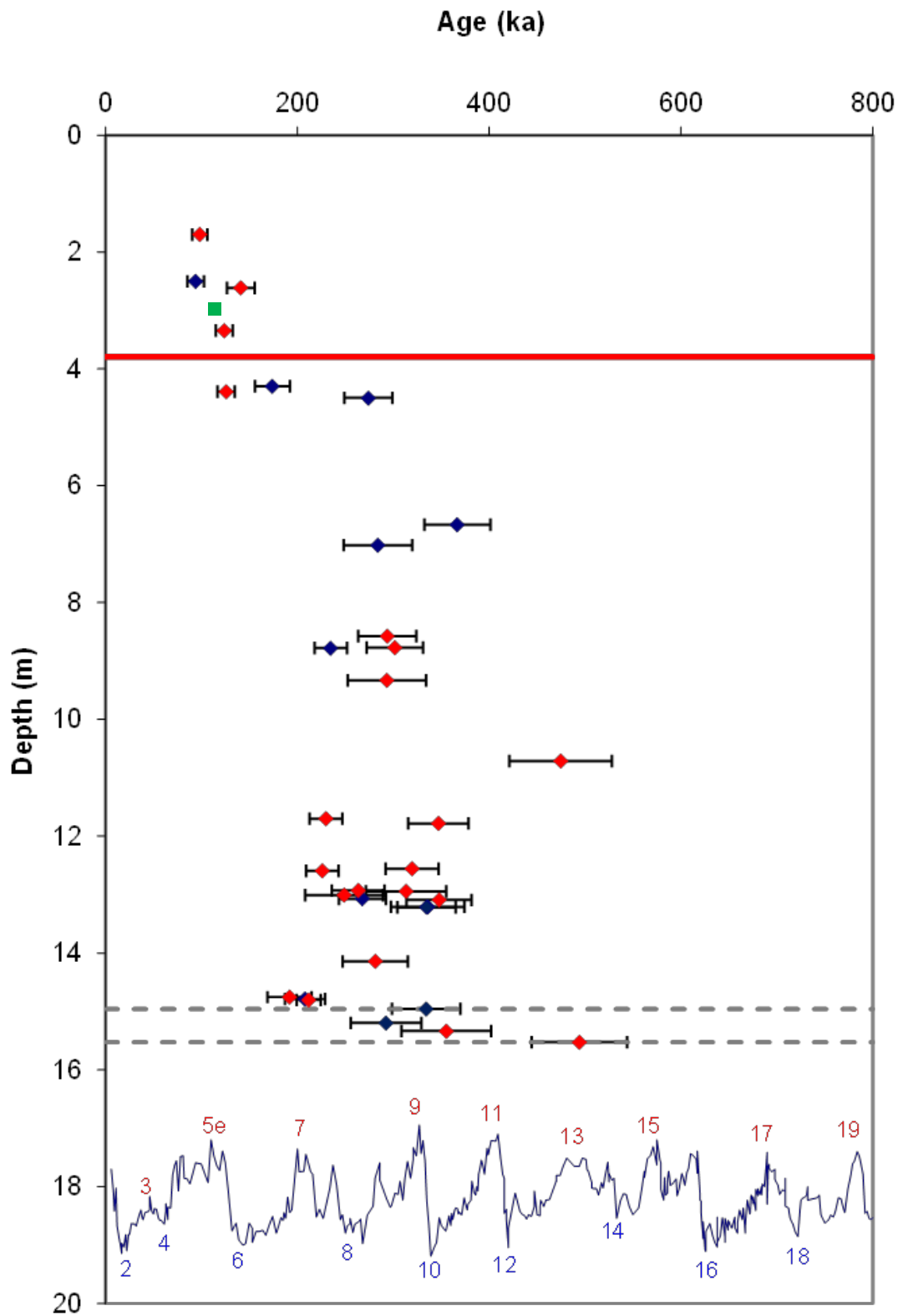


Figure 8

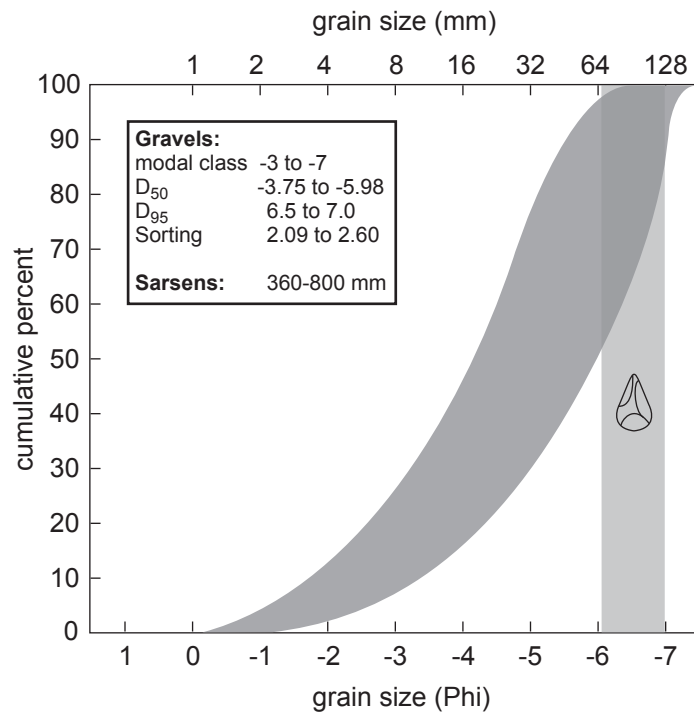
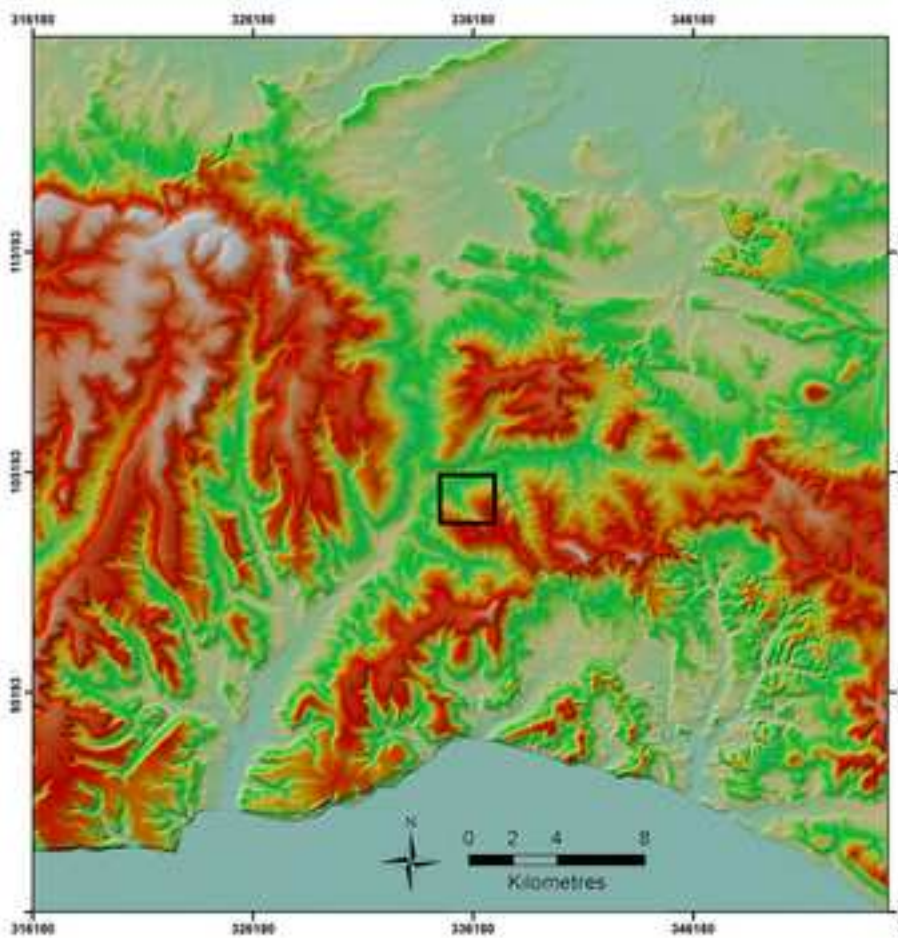


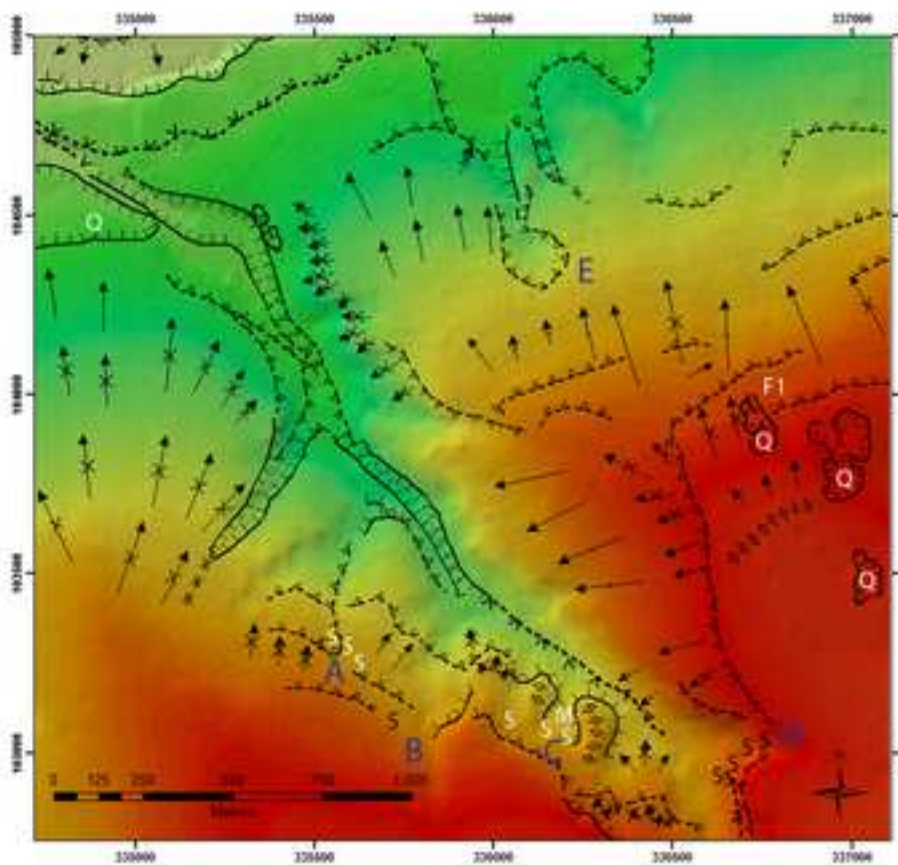
Figure 9

[Click here to download high resolution image](#)



Background

Shaded Relief DTM of
Digimap Ordnance Survey
Landform Profile Data
1:10,000 under licence to
University of Southampton
Displayed as RGB.
Upper image:
High (White-Grey: 316 m) &
Low (Pale Blue: 0 m)
Lower image:
High (Red: 279 m) &
Low (Green: 13.7 m)
Values determined by raster
extent.



Legend

- Concave slope unit
 - Rectilinear slope unit
 - Convex slope unit
 - ..V.. Smooth change of slope, concave
 - ▭▭▭ Abrupt break of slope
 - △△△ Smooth change of slope, convex
 - ◇◇◇ Rounded ridge crest
 - ≡≡≡ Rounded valley axis
 - Q Quarry
 - S Spring
 - M Spring mire
 - F1 Lithic Find 1
- Blue letters referred to in text

Figure 10

